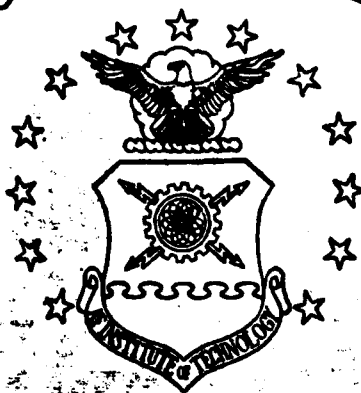






AD A124741

# AIR FORCE INSTITUTE OF TECHNOLOGY



AIR UNIVERSITY  
UNITED STATES AIR FORCE

INVESTIGATION OF AN IMPROVED FINITE ELEMENT  
MODEL FOR A REPAIRED T-38 HORIZONTAL  
STABILIZER FLUTTER ANALYSIS USING NASTRAN

THESIS

SCHOOL OF ENGINEERING

WRIGHT-PATTERSON AIR FORCE BASE, OHIO

DTIC FILE COPY

DTIC  
SELECTED  
1983 1983

This document was prepared  
for public release and its  
distribution is unlimited.

83 02 022114

①

AFIT/GAE/AA/82D-19

INVESTIGATION OF AN IMPROVED FINITE ELEMENT  
MODEL FOR A REPAIRED T-38 HORIZONTAL  
STABILIZER FLUTTER ANALYSIS USING NASTRAN  
THESIS

AFIT/GAE/AA/82D-19

George G. London, Jr.  
Capt USAF

Approved for public release; distribution unlimited.

SPIC  
S  
E

AFIT/GAE/AA/82D-19

INVESTIGATION OF AN IMPROVED FINITE ELEMENT  
MODEL FOR A REPAIRED T-38 HORIZONTAL STABILIZER  
FLUTTER ANALYSIS USING NASTRAN

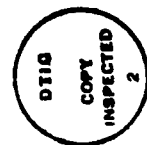
THESIS

Presented to the Faculty of the School of Engineering  
of the Air Force Institute of Technology  
Air University  
in Partial Fulfillment of the  
Requirements for the Degree of  
Master of Science

by  
George G. London Jr., B.S.M.E.  
Capt USAF  
Graduate Aerospace Engineering  
December 1982

Accession For	
NTIS GRA&I	<input checked="" type="checkbox"/>
DTIC TAB	<input type="checkbox"/>
Unannounced	<input type="checkbox"/>
Justification	
By _____	
Distribution/ _____	
Availability Codes	
Dist	Avail and/or Special
A	

Approved for public release; distribution unlimited.



## Preface

I thank my thesis advisor, Captain Hugh C. Briggs, whose guidance and interest in this thesis inspired me to select and enjoy this project. I am honored to have worked with such an advisor.

I wish to thank the many personnel of the Flight Dynamics Laboratory, in particular, Mr. J. Johnson, Mr. S. Pollock, Mr. L. Huttzell, and Mr. T. Noll, for their interest and support in the use of NASTRAN and various aerodynamic theories.

To my wife, ALFREDIA, I extend a special thanks for her understanding and support throughout the period of study. Appreciation goes to my daughters, Tamica and Myeshia, for leaving Dad to his studies.

Lastly, I would like to extend a warm thanks to my typist, Linda Kaye, whose professionalism is obvious from this work.

George G. London, Jr.

Contents

	<u>Page</u>
Preface. . . . .	ii
List of Figures. . . . .	iv
List of Tables . . . . .	vi
Abstract . . . . .	vii
I. Introduction . . . . .	1
Background. . . . .	1
Problem Statement . . . . .	5
Solution Approach . . . . .	5
II. Normal Modes Analysis. . . . .	8
III. Flutter Analysis Using Doublet Lattice . . . . .	13
IV. Flutter Analysis of a Repaired Model Using Doublet Lattice. . . . .	20
V. Flutter Analysis Using Strip Theory. . . . .	23
VI. Flutter Analysis Using Mach Box. . . . .	25
VII. Results. . . . .	28
VIII. Conclusions. . . . .	30
Bibliography . . . . .	32
VITA . . . . .	35

List of Figures

<u>Figure</u>		<u>Page</u>
1	T-38 Series 3 Stabilizer. . . . .	36
2	NASTRAN Structural Model. . . . .	37
3	First Bending, 17.36 cps. . . . .	38
4	Drag, 17.44 cps . . . . .	39
5	First Torsion, 44.42 cps. . . . .	40
6	Second Bending, 77.58 cps . . . . .	41
7	Second Torsion, 119.15 cps. . . . .	42
8	Third Bending, 124.68 cps . . . . .	43
9	Third Torsion, 170.38 . . . . .	44
10	8 by 8 Doublet Lattice Aerodynamic Model of Stabilizer. . . . .	45
11	144 Grid Point Model for Input to Spline. . . . .	46
12	V-G Diagram of Computed First Three Modes . . . . .	47
13	NAI's V-G Diagram of Computed First Three Modes . . . . .	48
14	V-G Diagram of Modes 4 to 6 . . . . .	49
15	Frequency vs. Velocity, First 6 Modes . . . . .	50
16	Segmented Spline, Inboard and Outboard Sections . . . . .	51
17	Segmented Spline, Inboard Forward and Aft, Outboard Forward and Aft . . . . .	52
18	15 Grid Point Model for Input to Spline . . . . .	53
19	Simulated Repair, Hole Trailing Edge. . . . .	54
20	Simulated Repair, Hole Tip. . . . .	55
21	Simulated Repair, Delamination Leading Edge . . . . .	56

List of Figures (Cont'd.)

<u>Figure</u>		<u>Page</u>
22	Repair Limit, Hole Trailing Edge. . . . .	57
23	Repair Limit, Hole Tip. . . . .	58
24,25	Repair Limit, Delamination. . . . .	59
26	Simulated Repair Strip, Rib to Rib. . . . .	60
27	Strip Theory Aerodynamic Model of Stabilizer. . . . .	61
28	Regions of Mach Box Aerodynamic Model . . . . .	62
29	Mach Box Aerodynamic Model of Stabilizer. . . . .	63

List of Tables

<u>Table</u>		<u>Page</u>
I	Comparison of First Three Modes of Vibration. . . . .	9
II	Results of Normal Modes Analysis Without ASET . . . . .	11
III	Results of Normal Modes Analysis With ASET. . . . .	11
IV	Frequency Changes Due to Spring Constant Changes. . . . .	12
V	Flutter Speed Changes Due to Spring Constant Change . . . . .	16
VI	Flutter Speed Changes Due to Variation of K . . . . .	19
VII	Flutter Speed Changes Due to Repairs. . . . .	21
VIII	Strip Theory Flutter Conditions After Repair. . . . .	24
IX	Mach Box Flutter Conditions . . . . .	26
X	Mach Box Flutter Conditions After Repair. . . . .	27

Abstract

This thesis investigates the use of an improved finite element model of a T-38 horizontal stabilizer for flutter analysis using NASTRAN. The procedure for evaluating the effect of repairs on the flutter speed is developed and its sensitivity to several modeling assumptions and practices is presented. The procedure is to be used by Air Force engineers to evaluate repair limits of T-38 stabs.

The NASTRAN flutter speed calculations are based upon a structural model, an unsteady aerodynamic model and an interface model (splines). The structural model consists of a flat array of plates and bars representing the single spar honeycomb structure. A flat array of doublet lattice panels were chosen for the unsteady aerodynamic model. An interface between these two models is required to find the down washes on the aerodynamic model due to motion of the structural model. This is accomplished by interpolation via surface splines.

Solution sensitivity to various parameters were considered to determine their effect on the flutter conditions. In addition to using the doublet lattice method, strip theory and mach box methods were used in the flutter analysis. This allowed a comparison of flutter conditions versus aerodynamic theory to be made.

Abstract (Cont'd.)

The results show that the current repair limits have little or no effect on the flutter conditions, therefore the procedures presented in this investigation should be used to establish new repair limitations.

INVESTIGATION OF AN IMPROVED FINITE ELEMENT  
MODEL FOR A REPAIRED T-38 HORIZONTAL  
STABILIZER FLUTTER ANALYSIS USING NASTRAN

I. INTRODUCTION

Background

San Antonio Air Logistics Center (SAALC) has the primary responsibility for all engineering and maintenance for the Northrop/United States Air Force T-38 Talon supersonic jet trainer. This responsibility includes determining whether or not a damaged T-38 stabilizer (stab) can be repaired within the limits stated in the T.O. IT-38A-3. Because the stab (Fig. 1) is a flutter critical component on the aircraft, the repair limits are established based on changes to the flutter speed. SAALC currently uses a method that conservatively predicts flutter speeds. To improve their flutter speed predictions, SAALC began an investigation, in 1975, for a more accurate analysis. The investigation was subsequently passed on to the Air Force Institute of Technology (AFIT) master of science students.

In 1979, Lassiter (Ref 5) began his investigation into the initial development of a structural model for use in flutter analysis using NASA Structural Analysis (NASTRAN). Lassiter's structural model consisted of two dimensional quadrilateral plate and bar elements. The finite element structural model was found to be lacking in stiffness.

The weight, center of gravity, and mass distribution of the model agreed fairly well with that of the actual stab. Lassiter conducted rigid and flexible root analysis of the model and compared the results with calculated data from Northrop Aircraft Incorporation (NAI). The results from the modal analysis showed good representations of the mode shapes but some of the frequencies varied as much as 20 cycles per second (cps). Lassiter used the finite element model with the above-mentioned discrepancies to perform a flutter analysis which yielded a flutter speed that was well below the NAI-reported flutter speed. The NAI 57-59 report stated that the series two and series three stabs have the same stiffness and Lassiter's model of a series three stab was found lacking stiffness. Since most of the previous analyses and tests by NAI were done on a series two stab, further investigation was necessary on the series three stab.

Thomson (Ref 18) worked to verify the series three finite element model under static loads, performed vibration tests on a stab, accomplished a NASTRAN modal analysis on a series three model, and performed a NASTRAN flutter analysis. The series two and three stabs were modeled for static load comparison and both lacked stiffness when compared with NAI's experimental results. The series three model lacked more in stiffness, causing Thomson to increase the elastic and shear moduli by 30 percent. The calculated frequencies between the series two and three models were very close to each other and the mode shapes were good representations of his experimental mode shapes.

For verification of a steady aerodynamic model, Thomson made a comparison between USSAERO and NASTRAN models, and preliminary experimental data. There was good correlation between the models and the experimental data. Thomson concluded that NASTRAN modeled the aerodynamics of the airfoil correctly for the steady case. The results of his flutter analysis was well below reported flutter speeds. Thomson recommended that corrections to the model (tuning) should be accomplished and the torsional spring stiffness of the hydraulic actuator system should be investigated.

Sawdy (Ref 17) used Thomson's two-dimensional model for the prediction of static displacement for the T-38 stab. He completed experimental static deflection tests on the series three stab and performed a static analysis on the finite element model. The experimental test set-up for the stab measured the displacements for ten load conditions with the displacements measured at twenty-five locations for each loading condition. The test paralleled that developed by Northrop for the series two stab with deviations in pad size, several load conditions, the use of a load cell in place of the control system actuator ram, and boundary conditions. Because of these differences, a good comparison of the static analysis of the series two and series three stabs could not be accomplished. He explained the use of optimization theory for tuning the finite element model based upon the static displacements found during his experimental tests. A value of  $1.18 \times 10^6$  in-lb/rad for modeling the load cell was found by direct search to produce the lowest

error value. With the combined optimum torque tube bending inertia and actuator arm spring constant, the error was found to be 1.6 compared to 10.4 before any optimization attempts. Sawdy concluded that the finite element model using orthotropic plate elements represents a good stabilizer finite element model.

Concurrent with Sawdy's investigation, Dodge (Ref 2) began improving the structural model's frequency response. Flutter analysis requires accurate mode shapes and frequencies from the model. This is accomplished by adjusting (tuning) the model to match the characteristics of the actual stab. The modulus of elasticity and shear modulus were the material properties chosen by Dodge for tuning the model. The cross-sectional properties chosen were the bending and polar moments of inertia of the spar, trailing edge and leading edge elements. Changing the structural mass and varying the airfoil thickness were also chosen for a total of six parameters used in tuning the model. Dodge concluded that an increase of 37 percent in airfoil thickness was considered the best tuned model without changing the type or number of elements in the model. The airfoil thickness was found to affect the torsional and bending frequencies equally. Modeling of the control system pitch stiffness was found to affect the first torsion mode the most. This mode is considered by Northrop to be the most crucial mode because of its effect on the flutter speed. Dodge found a pitch spring constant

of  $4.40 \times 10^6$  in-lbs/rad was necessary to tune the model to NAI's first torsion mode. His best model was the result of increasing the airfoil thickness by 37 percent and using a control system spring constant of  $4.40 \times 10^6$  in-lbs/rad.

#### Statement of the Problem

Develop a procedure to select the aerodynamic model, structural model, and splines for use in the flutter analysis process with the goal of determining flutter speed changes of a repaired stab. This procedure is to be used by Air Force engineers for updating current repair limitations to the stab.

#### Solution Approach

A normal modes analysis was accomplished on Sawdy's and Dodge's best model in order to determine the most appropriate model to use in the investigation. The structural model chosen was the model used by Dodge (Fig. 2). A complete modal analysis of the model was accomplished to find the frequencies of vibration and mode shapes in the frequency region of interest. The aerodynamic model was chosen based on the requirements of the doublet lattice method. According to Huttshell (Ref 4), Noll (Ref 14), and Pollack (Ref 15), the doublet lattice method is considered the least conservative of all subsonic aerodynamic theories and it is used as a standard in industry.

Eastep (Ref 3) states that the doublet lattice method is preferred over other available methods and it is also considered less conservative when compared with the supersonic theories in the low supersonic range. If the aerodynamic theory is changed, the aerodynamic model must be changed. The required interface between the structural and aerodynamic models is the spline. The spline is the model chosen to find the down washes at the intersection of the aerodynamic panels (aero points) due to motion at the structural grid points and the spline chosen is dependent upon the aerodynamic theory used.

Using the above described models, the NASTRAN flutter procedure was used to determine the flutter speed and frequency. The flutter conditions obtained only approximate to the actual flutter conditions. The actual flutter conditions are obtained using an iterative procedure called match pointing. The actual flutter speed and frequency are obtained by varying the assumed mach number and reduced frequency until the mach number at flutter matches the assumed mach number. Huttzell, Noll, and Pollack state that the general practice is to match point if the predicted flutter conditions are close to the operational limits of the aircraft, including a 15 percent safety factor. If the flutter conditions are not close to these limits, match pointing is not accomplished. This practice is to be followed during this investigation.

After determining the flutter conditions, various input parameters were changed to determine changes in the predicted flutter conditions. Once this information was obtained, mass was added to the structural model to simulate a repaired stabilizer and the flutter procedure was repeated. In addition to these procedures, strip theory and the mach box methods were used to obtain a comparison between aerodynamic theories and flutter conditions. The aerodynamic model was changed and the process repeated for these theories. Simulated repairs were accomplished by changing the structural model and the flutter procedure repeated to determine changed flutter conditions for the stab using both theories.

## II. NORMAL MODES ANALYSIS

Modal analysis is a necessary step that must be performed before attempting a flutter analysis. The frequencies and mode shapes of the NASTRAN structural model were calculated and compared with the results obtained by NAI calculations (Ref 9) and NAI's experimental data (Ref 8) of the stab using the flexible root installed boundary conditions. Also, modal analysis is performed to determine the modes eliminated and modified by applying Guyan reduction. The remaining frequencies and mode shapes are then used by NASTRAN in the flutter analysis procedure. A brief discussion of NASTRAN's modal analysis is necessary.

Rigid Format Three (Ref 13) and the displacement approach is used for the normal modes analysis. The four methods of algebraic eigenvalue extraction available using NASTRAN are the tridiagonal, determinant, inverse power, and the Upper Hessenberg. The inverse power method was chosen because the eigenvalues and eigenvectors could be found at the same time. As a tracking method, the inverse power method extracts the roots, one at a time, by iterative procedures applied to the original dynamic matrices. For the inverse power method, the eigenvalue problem is stated as

$$[K - \lambda M] \{U\} = 0$$

where K is a stiffness matrix, M is a mass matrix, and U is a displacement vector, and  $\lambda$  is the square of the natural frequency. With the aid of GCSNAST (Ref 6), the mode shapes can be depicted graphically.

For all present analyses, the NASTRAN structural model used is the best model by Dodge, unless otherwise stated. A normal modes analysis was performed and the results were compared to NAI calculated and experimental data and results of Eglin's Ground Vibration Tests (GVT) (Ref 16). These results, based on the installed boundary conditions, are listed in Table I.

Table I  
Comparison of the First Three Vibration Modes

<u>Mode</u>	<u>Eglin's GVT Freq (cps)</u>	<u>NAI Computed Freq (cps)</u>	<u>NAI Experimental Freq (cps)</u>	<u>NASTRAN Freq (cps)</u>
1st Bending	18.52	17.61	17.3	17.37
1st Torsion	50.20	44.89	44.9	44.33
2nd Bending	70.69	78.76	71.7	77.64

The results from NASTRAN compare favorably with the NAI calculated and experimental data. These results imply that the structural model has

been tuned to match the characteristics of the actual stab.

Knowing what modes are used in the flutter analysis process is very important to ensure no unintended modes are used. This check is best accomplished using the normal modes analysis. The frequency range of interest is given as input data and the resulting frequencies and their order of extraction are listed. The importance of the extraction order is best presented by an example. If three of the frequencies were 119, 124, and 170 cycles per second and their extraction order was 124, 119, and 170, the 119 cps would not be included in the flutter analysis if the upper limit was 100. This is because NASTRAN will find all values in the range, 0 to 100, and one value out of that range (124) which is calculated first. The frequency of 119 cps could be included in the flutter analysis and would appear as an unknown mode to the user.

NASTRAN's flutter analysis procedure does not allow the use of all degrees of freedom. The unwanted degrees of freedom are eliminated by using the Guyan reduction procedure. The lateral displacement was the only degree of freedom retained for flutter computations. The normal modes analysis was repeated with and without application of Guyan reduction to determine the extraction order, modes eliminated, and the frequencies that were changed. These results are listed in Tables II and III and shown in Figures 3 through 9.

Table II  
Normal Modes Analysis Without Using Guyan Reduction

<u>Mode #</u>	<u>Mode</u>	<u>Extraction Order</u>	<u>Frequency (cps)</u>
1	1st Bending	4	17.36
2	Drag	3	17.44
3	1st Torsion	2	44.42
4	2nd Bending	1	77.58
5	2nd Torsion	6	119.15
6	3rd Bending	5	124.68
7	3rd Torsion	7	170.38

Table III  
Normal Modes Analysis Using Guyan Reduction

<u>Mode #</u>	<u>Mode</u>	<u>Extraction Order</u>	<u>Frequency (cps)</u>
1	1st Bending	3	17.37
2	1st Torsion	2	44.33
3	2nd Bending	1	77.64
4	2nd Torsion	5	119.07
5	3rd Bending	4	124.67
6	3rd Torsion	6	171.73

The drag mode (Fig. 4) was eliminated using Guyan reduction, but the other frequencies show no significant change. This mode is referred to as the drag mode because it is the deformation that is parallel to the wind direction.

The first torsion mode was reported by NAI (Ref 9) to be the flutter critical mode and it is the mode that is directly affected by changes in the control system pitch stiffness. Variations in control system pitch stiffness were accomplished to determine the first torsional modes sensitivity to this parameter. Two of the values used were  $1.72 \times 10^6$  in-lbs/rad based upon bench tests of the control system actuator by NAI (Ref 10) and  $4.4 \times 10^6$  in-lbs/rad from the model tuning by Dodge. Unless otherwise specified, Dodge's value of  $4.4 \times 10^6$  in-lbs/rad is used for all flutter analyses. Table IV lists the changes in the first torsion frequency due to changes in the modeled control system pitch stiffness.

Table IV  
1st Torsion Frequency Change Due to Spring Constant Change

<u>Spring Constant (<math>10^6</math>)</u>	<u>Frequency (cps)</u>
1.00	29.36
1.18	31.08
1.72	35.11
2.00	36.73
3.00	40.87
4.40	44.33

### III. FLUTTER ANALYSIS USING DOUBLET LATTICE METHOD

In addition to the structural model, one of the most important factors in flutter analysis is the aerodynamic model. The attributes of a good aerodynamic model depend on the aerodynamic theory used. With NASTRAN, there are five aerodynamic theories available; all assume small amplitude sinusoidal motions and the transient aerodynamic forces are obtained by fourier methods. The aerodynamic analysis is based on the finite element approach in the same manner as structural analysis. The finite elements are strips or boxes for which there are aerodynamic forces. The lattice methods utilize arrays of trapezoidal boxes whose sides are parallel to the airflow.

According to Ref 12, the aspect ratio of the trapezoidal boxes should be less than 0.08 times the velocity divided by the greatest frequency of interest, but no less than four boxes per chord should be used. This led to an aerodynamic model consisting of eight chordwise and eight spanwise boxes (Fig. 10). The stab is, therefore, modeled as a flat doublet panel, divided into an eight by eight array of boxes. With the structural and aerodynamic models chosen, the interface model can be selected.

Choosing the proper interface model is another important factor in the flutter analysis process. This interface is based upon the theory of splines (Ref 12). High aspect ratio or beam models require

the use of linear splines. Since the stabilizer is modeled as a flat plate, the use of surface splines was appropriate. Splines are used to find the down washes at the aero points due to motion at the structural points. All aero elements must be referred to by a spline or that element will have no wash. If desired, the spline can be segmented into any rectangular subarray of boxes on a panel. The input points to the spline are the desired structural grid points to be used in the analysis. With the spline defined, all models required for flutter analysis have been specified. These models, structural, aerodynamic, and splines, will not be changed in the analyses unless specifically stated.

Before the flutter analysis process can be used, the method of modal flutter analysis must be chosen. Modal flutter analysis methods available using NASTRAN are the K, KE, and PK. The K method allows looping through three sets of parameters: density ratio, mach number, and reduced frequency. The KE method, though more efficient than the K method, is restricted to no damping matrix and no eigenvector recovery. The PK method tracks the aerodynamic matrices as frequency dependent springs and dampers, where the frequency is estimated by the user and the eigenvalues are found. The K method was chosen because eigenvector recovery is available for mode shape description at the flutter condition. To determine the flutter condition, a plot of velocity (V) versus damping (g) for various reduced frequencies (k)

is accomplished to locate the point where the damping is zero. The velocity at this point is the flutter velocity ( $V_f$ ) and the frequency is the flutter frequency ( $\omega_f$ ).

Using the K method, the tuned structural model, the eight by eight aerodynamic model, and a surface spline with inputs from all structural nodes (Fig. 11), the flutter analysis process was accomplished. All analyses are based upon sea level conditions and .5 Mach unless stated otherwise. The flutter condition from the analysis was a  $V_f$  of 916 Knots and  $\omega_f$  of 29.7 cps. These results compared favorably with the NAI (Ref 11) reported  $V_f$  of 830 Knots and  $\omega_f$  of 29 cps. The report also stated that the 830 knot flutter speed was ten to twenty percent below expected values. A V-g diagram, at various values of reduced frequency, was plotted (Fig. 12) for the first three modes and compared to a similar plot by NAI (Fig. 13). Additionally, modes 4 through 6 were plotted on a V-g diagram (Fig. 14) as well as a plot for the first six frequencies versus velocity (Fig. 15). Figure 12 was almost identical to those produced by NAI but with the noted difference in flutter speed. NAI's 830 Knot  $V_f$  was based on three percent damping whereas the results in this report are based on zero damping.

Changes to these models and other input variables were investigated to determine their effect on  $V_f$ . These changes were varying the modeled control system pitch stiffness, segmenting the splines,

reducing the number of aerodynamic boxes, and varying the altitudes. The previously mentioned values for the control system pitch stiffness were used in the flutter analysis procedure to determine the effect on  $V_f$ . The results, listed in Table V, confirm the expected flutter speed changes due to a change in the first torsion frequency. The change in the first torsion frequency is directly effected by the control system pitch stiffness resulting in a flutter speed decrease as the torsional frequency decreases.

Table V  
 $V_f$  Changes Due to a Spring Constant Change

<u>Spring Constant</u>	<u>In Vacuum First Torsion Freq (cps)</u>	<u><math>V_f</math> (knots)</u>	<u><math>\omega_f</math> (cps)</u>
1.00	29.36	412	23.5
1.18	31.08	503	23.8
1.72	35.11	596	26.2
2.00	36.73	635	27.1
3.00	40.87	738	29.2
4.40	44.33	916	29.7

Segmenting the splines was investigated to determine if the computer memory requirements could be reduced and to determine flutter speed changes. The segmented splines were of two types: one consisting of inboard and outboard sections (Fig. 16) and the other consisting of inboard forward, inboard aft, outboard forward, and outboard aft sections (Fig. 17). All aerodynamic elements and all structural nodes were used as input to each spline. It was discovered that the flutter frequency and velocity did not change with either type of spline. The amount of computer memory required was reduced from 300K for a full spline to 200K for a segmented (inboard and outboard) spline, therefore, the user with limited computer resources could use this procedure if the splines are segmented. There was no additional memory reduction by further segmenting the spline. Also, a full spline with the number of structural grid points reduced to 15 (Fig. 18) was used with the result showing a reduction in flutter speed and no significant cost reduction.

Since Thomson (Ref 18) used an aerodynamic model consisting of 20 aerodynamic boxes compared to the 64 used here, it was necessary to determine the effect on  $V_f$  caused by such a model change. With this model change and using all structural nodes, the resulting flutter condition was a  $V_f$  of 846 Knots and  $\omega_f$  of 31.6 cps. This was a significant reduction from the 916 knot flutter speed previously discovered. The structural nodes input to the spline were reduced to 15 points and using the 20 box aero model, the flutter condition was a  $V_f$  of 855 Knots

and  $\omega_f$  was 30.4 cps. Again, the  $V_f$  of 855 knots was significantly below the 916 knot flutter speed. Based on these results, the 64 box aero model is the most appropriate model to use for flutter analysis.

To determine the effect on flutter speeds, the altitudes were varied and compared to the sea level conditions. Flutter will occur at one dynamic pressure  $q_f$ . Since  $q_f$  is  $\frac{1}{2}\rho_\infty V_f^2$ , the flutter dynamic pressure is considered a constant value. Therefore, as the altitude is increased,  $\rho_\infty$  (density of the free stream) will decrease and the flutter velocity must increase. Altitudes of 20,000 and 40,000 feet were used in the flutter analysis procedure resulting in  $V_f$  of 1127 Knots and  $\omega_f$  of 30.6 cps at 20,000 feet. Flutter conditions at 40,000 feet were not found using a reduced frequency range of .1 to 1.0. These results verify that  $V_f$  does increase with altitude.

The range of reduced frequency ( $k$ ), used in interpolation of the aerodynamic forces, was varied to determine if the flutter conditions were sensitive to that parameter. The initial values of  $k$  were selected such that no interpolation was required. The reduced frequencies selected were decreased to two values to span the region of  $k$  at flutter. This resulted in a decreased flutter speed with the flutter frequency remaining fairly constant. An increase in flutter speed resulted from using three values of  $k$  to span a region from .2 to .9k. The variation in flutter speed versus the range and number of  $k$  values used are listed in Table VI.

Table VI  
Flutter Speed Changes Due to Variation of k

<u>Number of k Values</u>	<u>Range of k</u>	<u>V<sub>f</sub> (knots)</u>	<u>ω<sub>f</sub> (cps)</u>
5	.15 - .25	916	29.7
3	.2 - .9	926	29.8
2	.2 - .6	883	30.4

The flutter conditions obtained using 5 values of k are considered to be the most accurate due to the fact that no interpolation was required when computing the aerodynamic forces at the values of k for the V-g plots.

All of the factors affecting V<sub>f</sub> have been investigated resulting in an aerodynamic model, structural model, and splines with the following characteristics: a spring constant of  $4.40 \times 10^6$  in-lbs/rad, a segmented spline consisting of an inboard and outboard section with input points local to each section, a sixty-four box aerodynamic model, and sea level conditions. Using these models, simulated repairs and their effects were investigated.

#### IV. FLUTTER ANALYSIS OF A REPAIRED MODEL USING THE DOUBLET LATTICE METHOD

To properly model the simulated repairs, the T.O. IT-38A-3 was used to find the current repair limitations and repair procedures. The repairs chosen for simulation were considered to be the ones that would change the flutter characteristics of the stab the most. The locations and types of damage simulated were a hole near the trailing edge (Fig. 19), a hole at the tip (Fig. 20), and delamination of the leading edge where some of the honeycomb core must be removed (Fig. 21). The size limitations for these areas (Ref. 19) are listed in Figures 22 to 25. The size simulated repairs were modeled to be close to the current repair limitations. The repairs were modeled by changing the non-structural mass of the elements in the depicted repair areas. The honeycomb core has a density of 3.1 lb per cubic foot and the repair material (Nylon phenolic core) has a density of 4.5 lb per cubic foot. The difference in the two densities was added to the repaired elements on the structural model. Due to the repair procedures, no additional mass was added for the skin patch. Using the changed structural model, the flutter analysis procedure was repeated.

The in vacuum frequencies of the repaired models changed very little from those of the clean model. Since the frequencies showed minor changes as a result of the repairs, there was no significant

change expected in the flutter conditions. Table VII shows a comparison of the clean model to the repaired models.

Table VII  
Comparison of Flutter Conditions of a Clean Model  
Versus Repaired Models Using Doublet Lattice

<u>Repair Type</u>	<u>In Vacuum 1st Torsion Freq (cps)</u>	<u><math>V_f</math> (knots)</u>	<u><math>\omega_f</math> (cps)</u>
Clean	44.336	916.540	29.762
Hole T.E.	44.334	916.468	29.764
Hole Tip	44.331	915.916	29.757
Delamination	44.302	919.384	29.677

With the modeled delamination, a slight increase in flutter speed was obtained. This was due to the mass addition forward of the elastic axis, which has a stabilizing effect. These results show that the flutter speed and frequency are not greatly affected by repairs within the current repair limitations.

A repair, which exceeded the current repair limitations, was modeled to investigate its changes to the flutter speed and frequency (Fig. 26). This repair was simulated by replacing the honeycomb core

with the repair core from the root rib to the tip rib in a section near the trailing edge. The results showed a flutter speed of 911 knots and a flutter frequency of 29.7 cps. Even though this repair exceeded current limitations, there was no significant change in the flutter conditions from that of a clean model.

## V. FLUTTER ANALYSIS USING STRIP THEORY

Utilizing the previously defined clean structural model, the aerodynamic model was changed to a strip theory model. Strip theory is an aerodynamic theory that uses strips parallel to the free stream direction to determine the aerodynamic data at subsonic and supersonic speeds. The aerodynamic model used to represent the stab consists of fifteen strips (Fig. 27). The spline must consist of a representation of all strips, therefore, the spline model and aerodynamic model are identical. All structural grid points (Fig. 11) were used as input points to the spline. With lift curve slope information along the span provided by NAI (Ref. 11), the flutter procedure was repeated.

The flutter analysis was accomplished at subsonic and supersonic speeds. There were no differences in the flutter conditions in either speed regime, therefore, the results stated are those computed at .5 Mach. The in vacuum first torsion frequency of 44.3 cps was changed to 29.04 cps at flutter with a flutter speed of 946 knots. The structural model was changed to simulate the previously defined repairs and the flutter procedure was repeated and the results are listed in Table VIII.

Table VIII  
Comparison of Flutter Conditions of a Clean Model  
Versus Repaired Models Using Strip Theory

<u>Repair</u>	<u>In Vacuum 1st Torsion Freq (cps)</u>	<u>V<sub>f</sub> (knots)</u>	<u>ω<sub>f</sub> (cps)</u>
Clean	44.3	946	29.04
Hole T.E.	44.3	946	29.04
Hole Tip	44.3	946	29.03
Delamination	44.3	947	28.98
Strip	44.2	943	28.98

The results in Table VIII showed the same trends found using the doublet lattice method including a slight increase in flutter speed for the delamination at the leading edge of the stab.

## VI. FLUTTER ANALYSIS USING MACH BOX

Another aerodynamic theory considered was the mach box method, a supersonic theory, which required a change in the aerodynamic model. The same clean structural model was used in this portion of the investigation. The mach box aerodynamic model consists of an array of rectangular boxes whose diagonals parallel the mach line (Ref 1). At the center of each box is a pulsating source emanating spherical disturbances. In general, the model, defined by the mach line and the planform, consists of the planform, diaphragm, and wake regions (Fig. 28). In NASTRAN, the user must specify the number of chordwise boxes and the mach number such that the number of boxes do not exceed 200. The aero model for the stab using the mach box method is shown in Fig. 29.

The spline must consist of at least three arbitrarily chosen points on the planform. Six locations were chosen on the stab to represent the spline model. Inputs from all structural nodes (Fig. 11) were used with the six spline points for use in the interpolation procedure.

Using sea level conditions and various mach numbers, the flutter procedure was repeated with the results listed in Table IX.

Table IX  
Flutter Conditions Using Mach Box

<u>Mach #</u>	<u>In Vacuum 1st Torsion Freq (cps)</u>	<u>V<sub>f</sub> (knots)</u>	<u>ω<sub>f</sub> (cps)</u>
1.10	44.3	X	X
1.15	44.3	X	X
1.20	44.3	X	X
3.0	44.3	790	46.7
5.0	44.3	780	46.7

The results show the flutter conditions at the higher mach numbers but no flutter conditions at mach number 1.2 and below even though the predicted flutter speed is within that region. The flutter frequency of 46.7 cps was not close to the expected value of 29 cps. Simulated repairs were made to the structural model and the flutter procedure repeated. The results show the same trend discovered using the doublet lattice and strip theories, but, the frequency is still far from the expected value. This data is based on an assumed Mach number of 3.0.

Table X  
Comparison of Flutter Conditions of a Clean Model  
Versus Repaired Models Using Mach Box

<u>Repair</u>	<u>In Vacuum 1st Torsion Freq (cps)</u>	<u>V<sub>f</sub> (knots)</u>	<u>ω<sub>f</sub> (cps)</u>
Clean	44.3	790	46.91
Hole T.E.	44.3	790	46.91
Hole Tip	44.3	789	46.91
Delamination	44.3	785	46.90
Strip	44.2	786	46.61

Unlike the strip and doublet lattice theories, the results due to delamination did not show an increase in the flutter speed. Even though mass was added forward of the elastic axis, the center of pressure is at 50 percent chord versus 25 percent chord, therefore, the result is a decrease in flutter speed. It is the author's conclusion that using the mach box theory, there are no flutter conditions in the region of interest.

## VII. RESULTS

The flutter speeds predicted in this report vary depending on the aerodynamic theory used. The results from the doublet lattice method are considered to be the most comparable to but still below actual. This is based upon a statement in Ref 12 that the computed 830 knot flutter speed is ten to twenty percent below the expected value. Also, the 830 knot flutter speed is based upon three percent damping while the computed flutter speeds in this report are based upon no damping. With the ten to twenty percent margin quoted, the flutter speed of the stab should be between 913 and 996 knots. The 916 knot  $V_f$ , predicted using doublet lattice method, is in the lower portion of this region and is considered a good estimate for the actual flutter speed. A flutter frequency of 29 cps was reported in reference 12, therefore, the  $\omega_f$  of 29.7 cps compares favorably to that value reported by NAI. With the simulated repairs used in the flutter analysis procedure, the flutter conditions were virtually unchanged from those of a clean model.

The results of this report were obtained by using procedures that deviated from those generally accepted for flutter analysis. A coarse aerodynamic model is usually chosen but it has been shown in this investigation that the flutter speed is sensitive to the size of the aero mesh and  $V_f$  may change by as much as 50 knots. Using all of the structural grid points as input to the spline versus a small number of

grid points, the change if  $V_f$  was not significant unless combined with the changes in the aero model. The best results were obtained using a fine aerodynamic model and all structural grid points. Segmenting the splines produced no change in flutter conditions, but resulted in a significant decrease in the amount of computer core memory required. This reduced computer requirement makes the procedures in this report available to a larger number of users. Also, the reduced frequency is usually chosen such that interpolation is required over much of the reduced frequency range. The flutter conditions show some inconsistencies depending on the range of  $k$  used, therefore, the  $k$  values should be chosen such that a minimal amount of interpolation for the aero forces is required.

### VIII. CONCLUSIONS AND RECOMMENDATIONS

The procedure used in this investigation for flutter analysis of clean and repaired models of the stab, ensure all factors affecting the flutter conditions are considered. According to Ref 7, an aircraft must be flutter free for up to 115 percent of the aircraft limiting airspeed. For the T-38, the limiting airspeed is 710 knots. Considering the safety margin required due to flutter, the aircraft should be flutter free up to an airspeed of 816 knots. From the results of this investigation, the changes in  $V_f$  due to the repairs are shown to be minor; therefore, it is recommended that the procedures in this report be used to determine the possibility of establishing new repair limitations for the stab. An additional safety factor can be added to the 916 knot speed to ensure that speed is not closely approached.

It is recommended that the flutter procedure be initiated using a coarse k set in order to determine the reduced frequency region at which flutter will occur. Since it has been shown that the flutter speed varies depending on the reduced frequency used, the coarse k set should be modified to a region in the vicinity of the expected reduced frequency at flutter. This modified k set should be chosen such that minimal interpolation for computation of the aerodynamic forces is required.

For establishing new repair limitations, it is recommended that the doublet lattice method be used. Within the current repair limitations, it appears as though strip theory gives the best results but as more mass is added near the trailing edge, there should be chordwise deformation and as a result, the flutter speed is affected. Chordwise deformation is not detected by strip theory, therefore, there is a larger decrease in flutter speed using strip theory when compared with the flutter speed decrease using the doublet lattice method.

### Bibliography

1. AFFDL-TR-68-30, Supersonic Unsteady Aerodynamics for Wings with Trailing Edge Control Surfaces and Folded Tips, Wright-Patterson AFB, OH: Air Force Flight Dynamics Laboratory, (AFFDL), August 1968.
2. Dodge, Lex C., Investigation of an Improved Structural Model for Damaged T-38 Horizontal Stabilizer Flutter Analysis Using NASTRAN, Wright-Patterson AFB, OH: Air Force Institute of Technology, December 1981.
3. Eastep, Franklin E., Faculty Member, Aeronautics and Astronautics Department, School of Engineering, Air Force Institute of Technology, (personal interview), Wright-Patterson AFB, OH: 16 July 1982.
4. Huttzell, Lawrence J., Aerospace Engineer, Flight Dynamics Laboratory (personal interview), Wright-Patterson AFB, OH: 17 August 1982.
5. Lassiter, John O., Initial Development for a Flutter Analysis of Damaged T-38 Horizontal Stabilizers Using NASTRAN, Wright-Patterson AFB, OH: Air Force Institute of Technology, March 1980.
6. McVinnie, Bill, et. al., GCSNAST Manual, Wright-Patterson AFB, OH: Engineering Systems Development Department, Technical Computer and Instrumentation Center, August 1979.

Bibliography (Cont'd.)

7. MIL-A-8870, Military Specification, Airplane Strength and Rigidity, Flutter, Divergence, and Other Aeroelastic Instabilities, Department of Defense, May 1980.
8. NAI-58-6, T-38A Vibration Mode Analyses of Empennage, Hawthorne, CA: Northrop Aircraft, Inc., June 1960.
9. NAI-58-11, T-38A Flutter Characteristic Summary, Vibration and Flutter Analysis, Hawthorne, CA: Northrop Aircraft, Inc., June 1960.
10. NAI-58-13, T-38 Vibration Mode Analyses of Wing, Hawthorne, CA: Northrop Aircraft, Inc., February 1959.
11. NAI-58-15, T-38A Flutter Analysis for Empennage, Hawthorne, CA: Northrop Aircraft, Inc., February 1960.
12. NASA SP-221(06), The NASTRAN Theoretical Manual, Washington, DC: Scientific and Technical Division, National Aeronautics and Space Administration, January 1981.
13. NASA SP-222(05), The NASTRAN User's Manual, Level 17.5, Washington, DC: Scientific and Technical Division, National Aeronautics and Space Administration, December 1978.
14. Noll, Tom E., Aerospace Engineer, Flight Dynamics Laboratory (personal interview), Wright-Patterson AFB, OH: 17 August 1982.
15. Pollack, Samuel J., Aerospace Engineer, Flight Dynamics Laboratory (personal interview), Wright-Patterson AFB, OH: 15 June 1982.

Bibliography (Cont'd.)

16. Rohlman, William H., CF-5 Horizontal Stabilizer Ground Vibration Test, Eglin AFB, FL: Structural Dynamics Laboratory, Air Force Armament Test Laboratory, (AFATL/DLJCS), October 1979.
17. Sawdy, Jack O., Investigation of a Two-Dimensional Model for the Prediction of Static Displacement for T-38 Horizontal Stabilators Using NASTRAN, Wright-Patterson AFB, OH: Air Force Institute of Technology, December 1981.
18. Thomson, Roger K., Investigation of an Improved Flutter Speed Prediction Technique for Damaged T-38 Horizontal Stabilators Using NASTRAN, Wright-Patterson AFB, OH: Air Force Institute of Technology, December 1980.
19. T.O. IT-38A-3, "Horizontal Stabilator Damage Repair," T-38 Maintenance and Repair Manual, Kelly AFB, Texas: San Antonio Air Logistics Center.

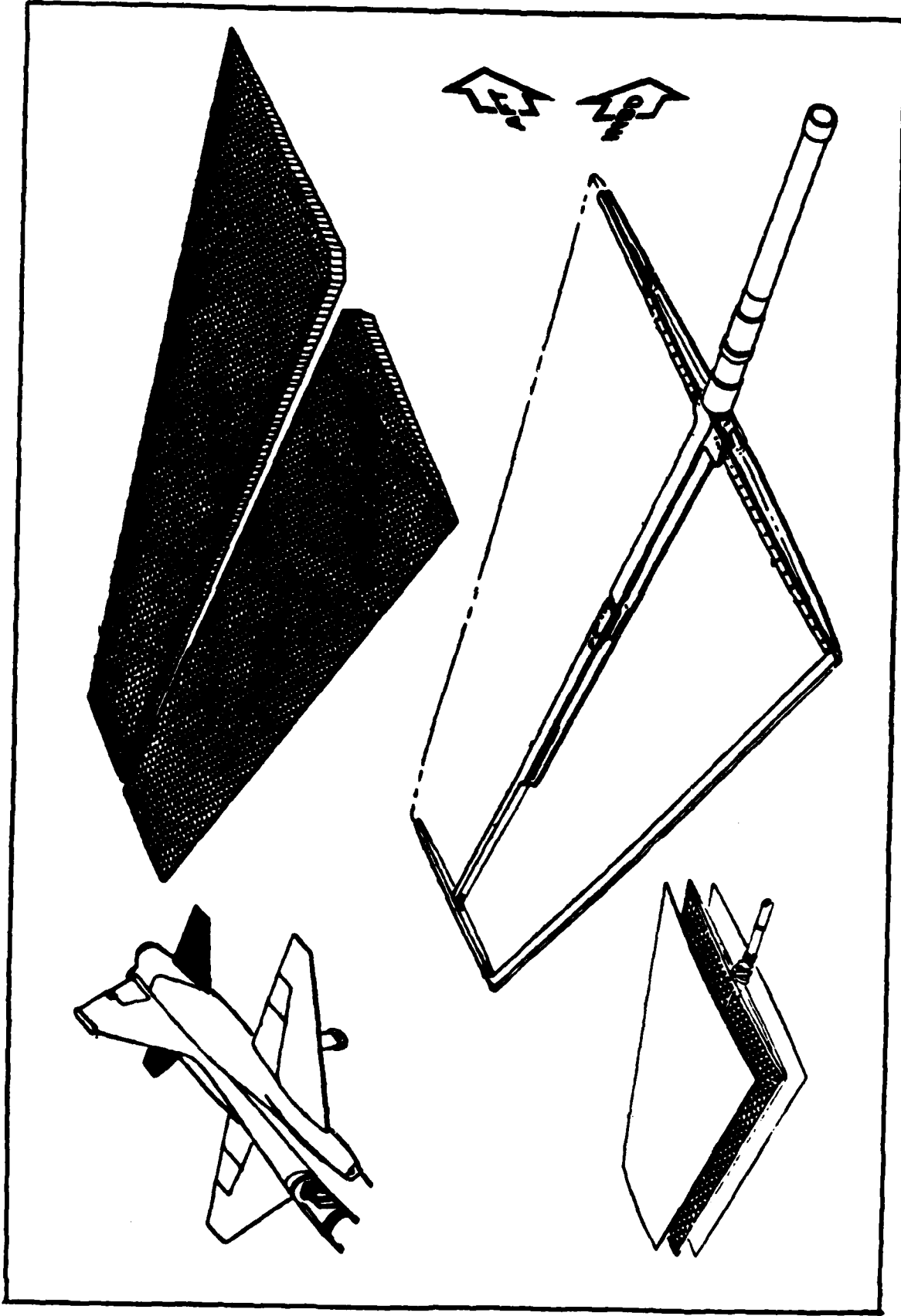


Figure 1 T-38 Series 3 Stabilizer (Ref 19)

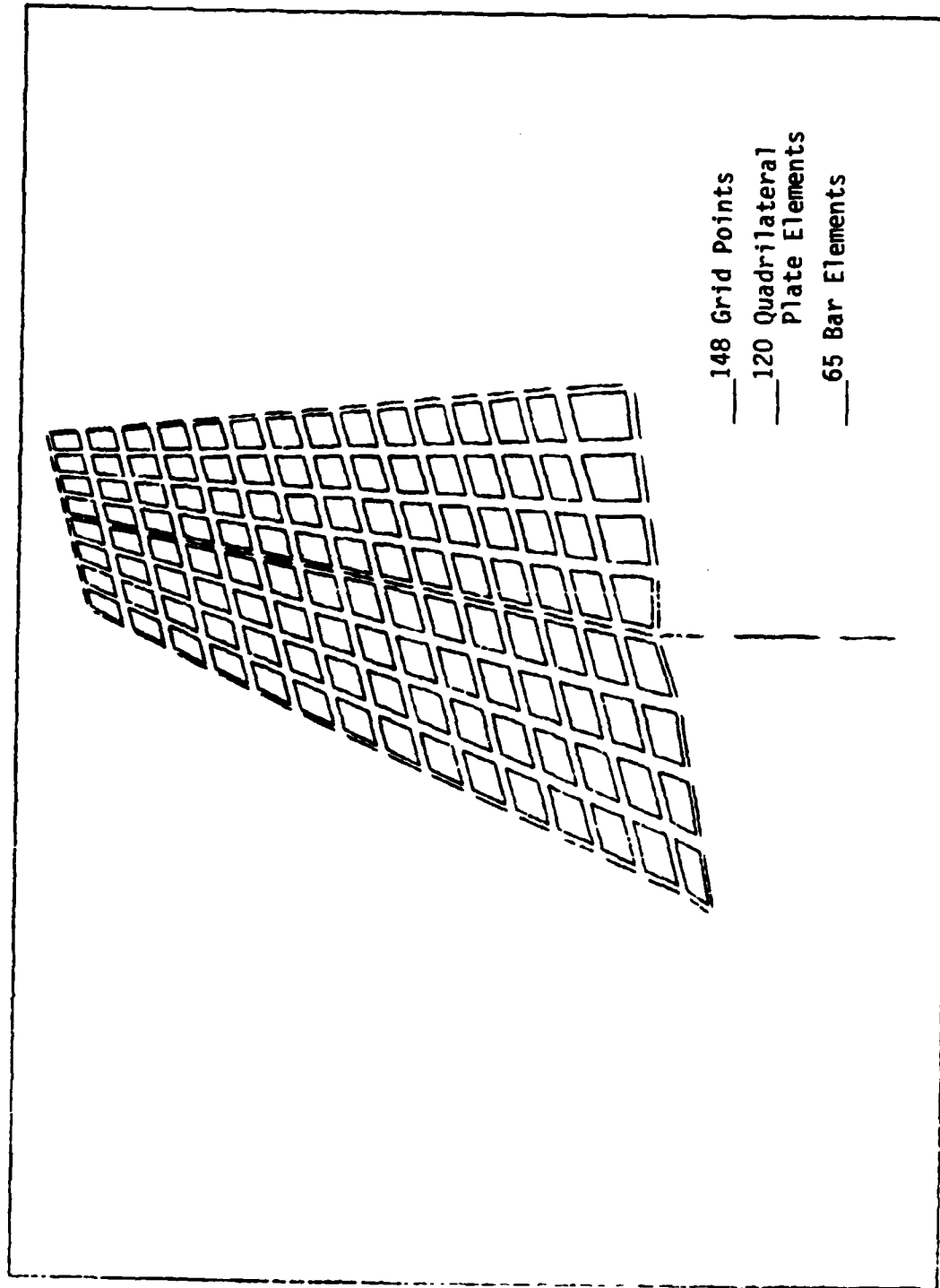


Figure 2 NASTRAN T-38 Series 3 Stabilizer Model

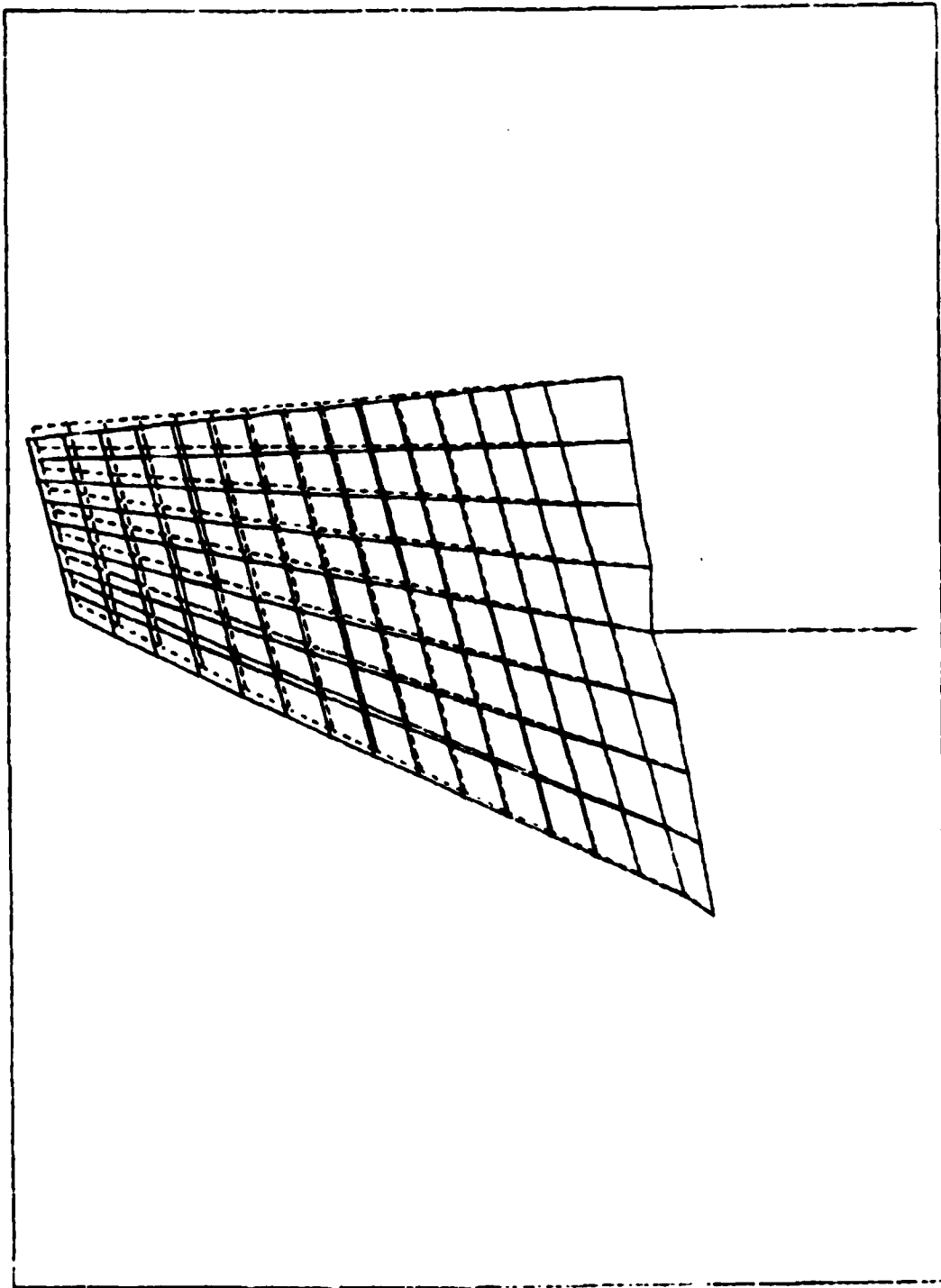


Figure 3 NASTRAN's 1st Bending Mode, 17.36 cps

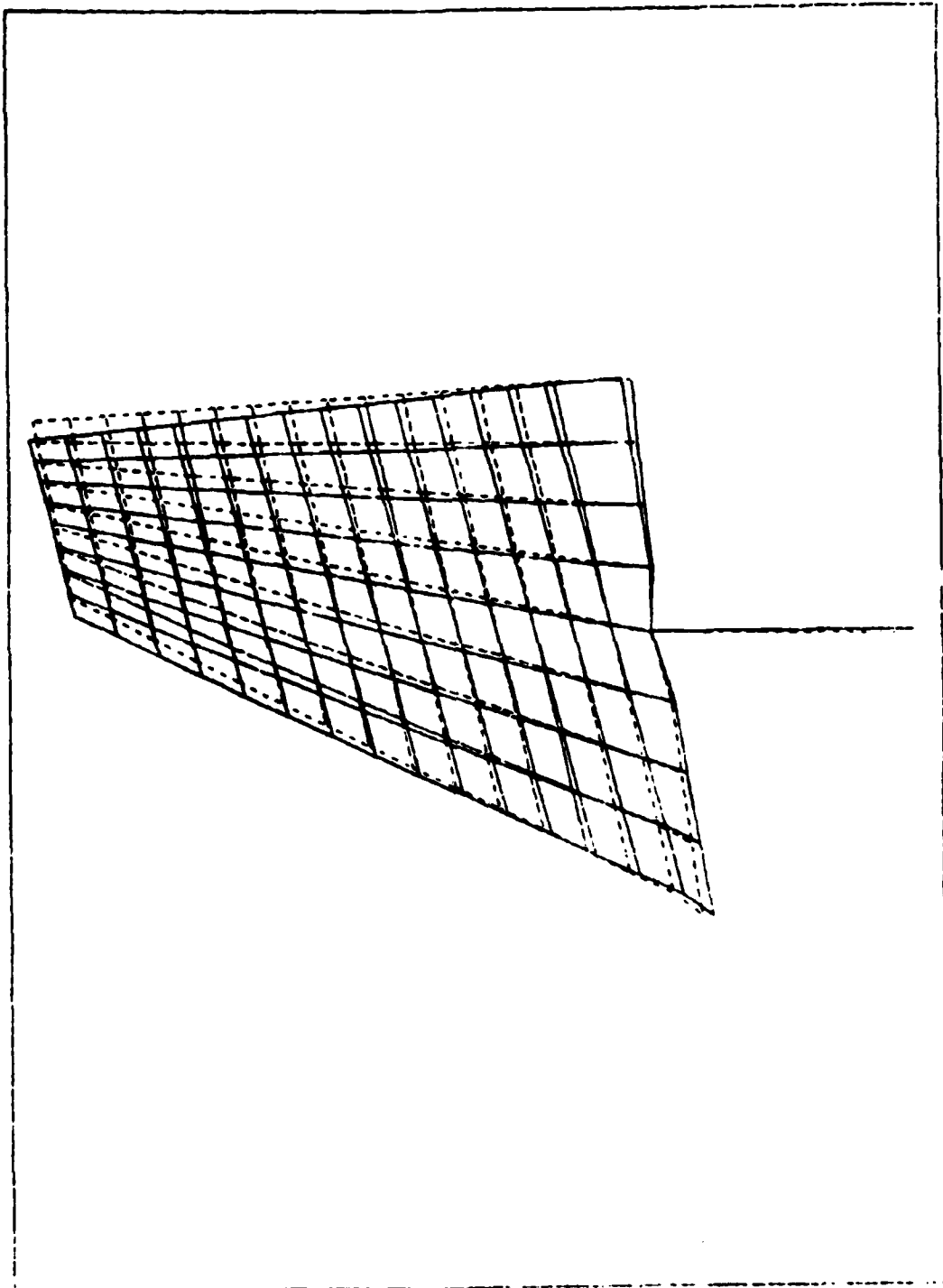


Figure 4 NASTRAN's Drag Mode, 17.44 cps

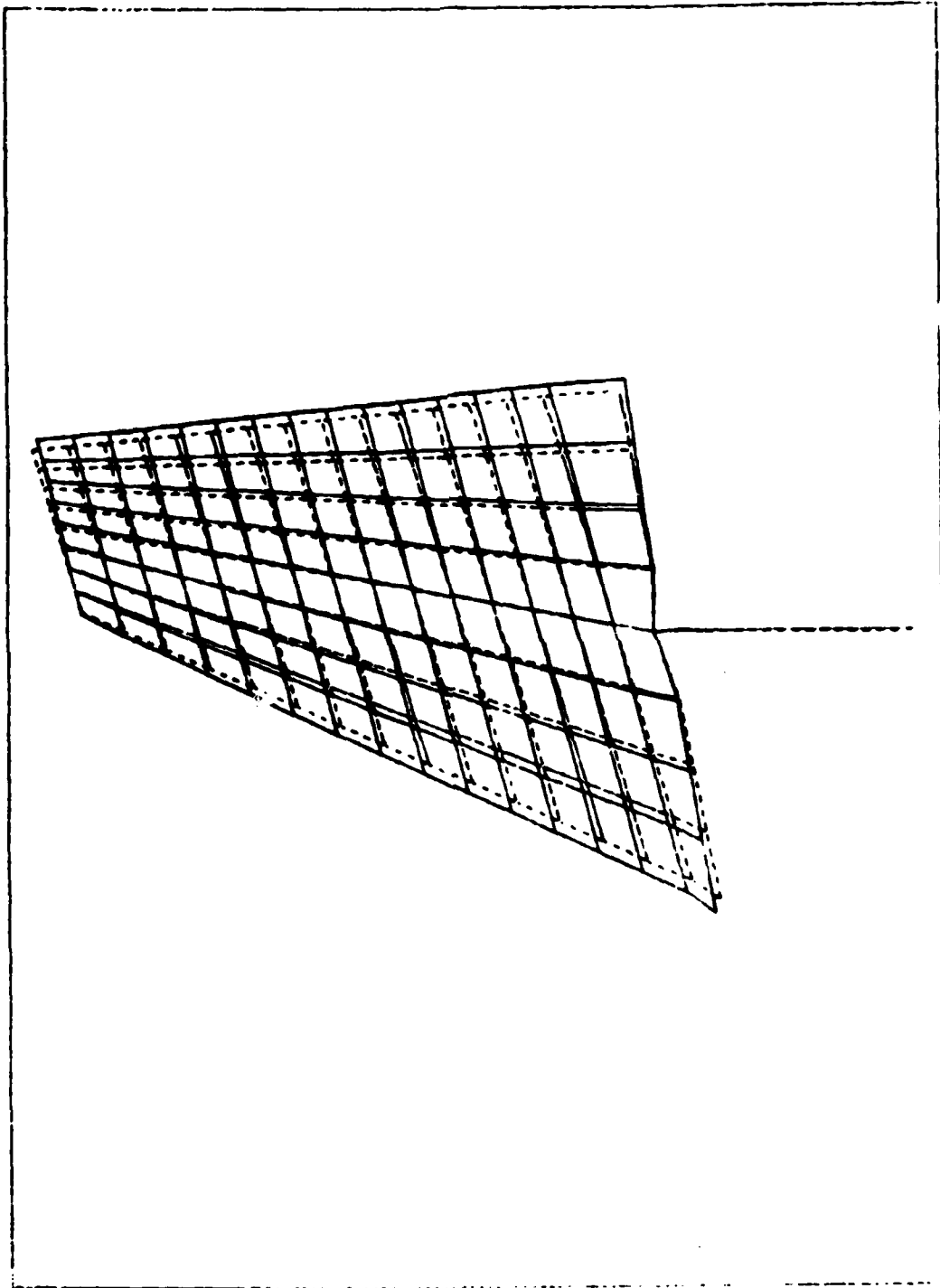


Figure 5 NASTRAN's 1st Torsion Mode, 44.42 cps

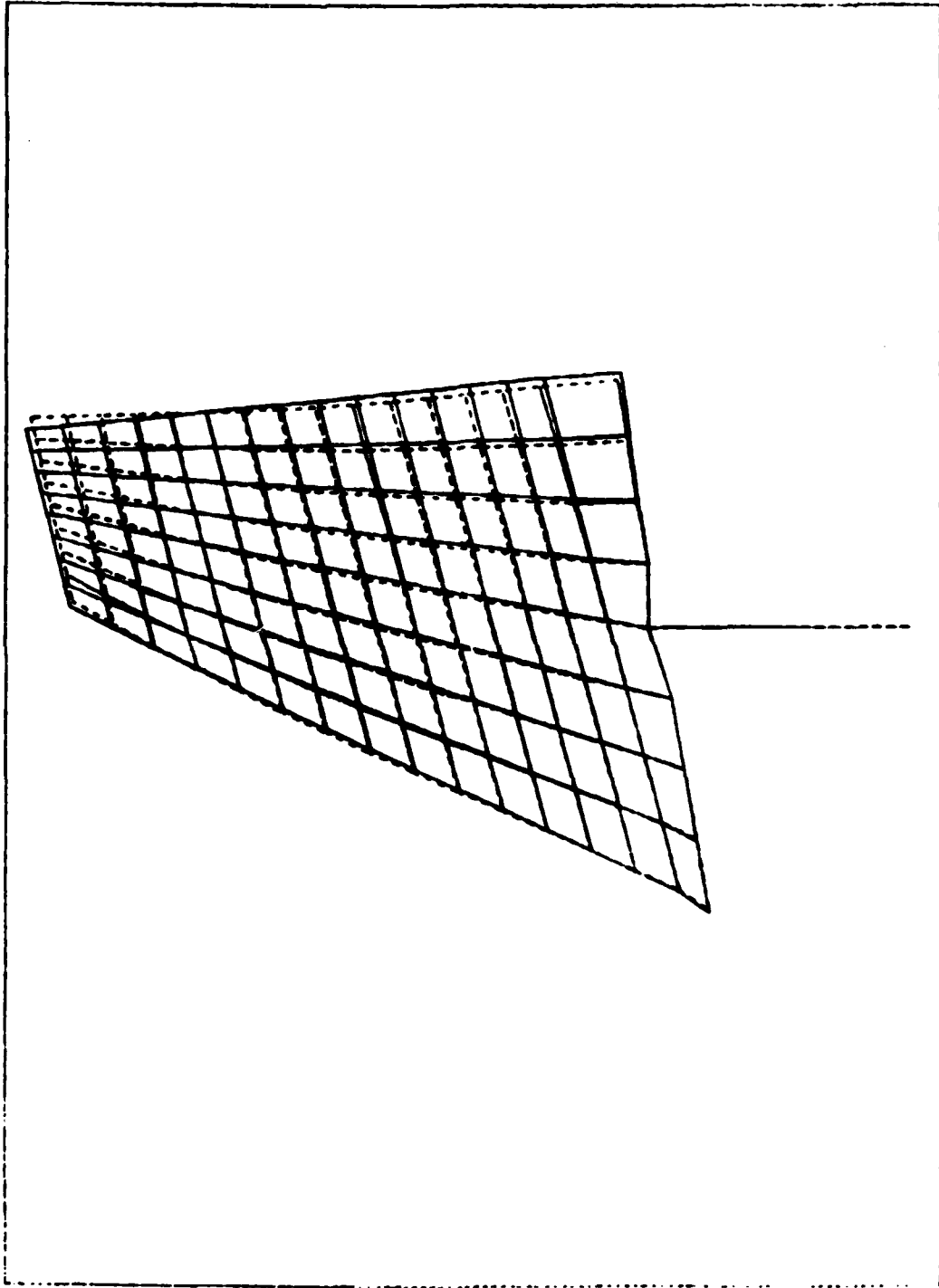


Figure 6 NASTRAN's 2nd Bending Mode, 77.58 cps

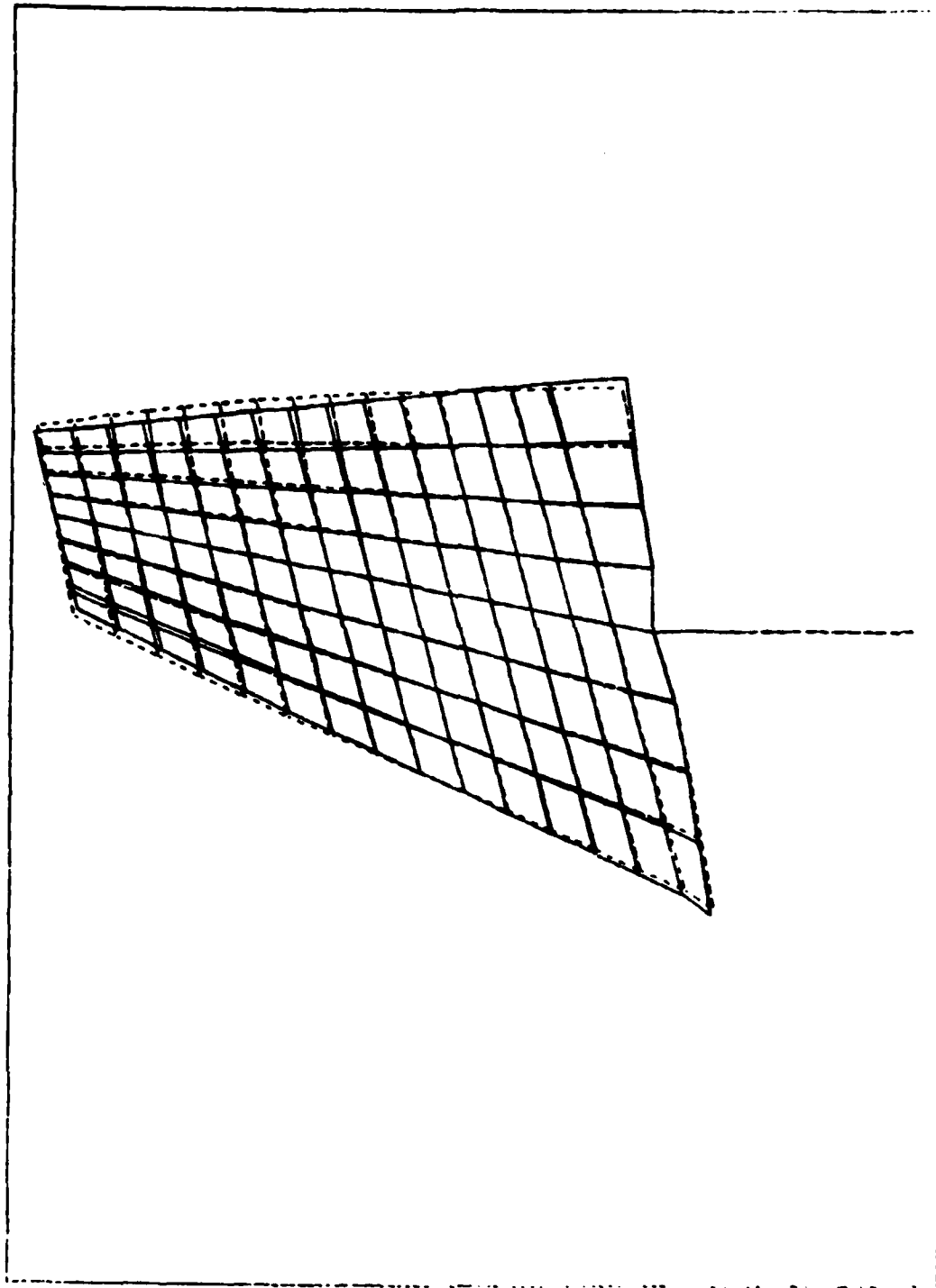


Figure 7 NASTRAN's 2nd Torsion Mode, 119.15 cps

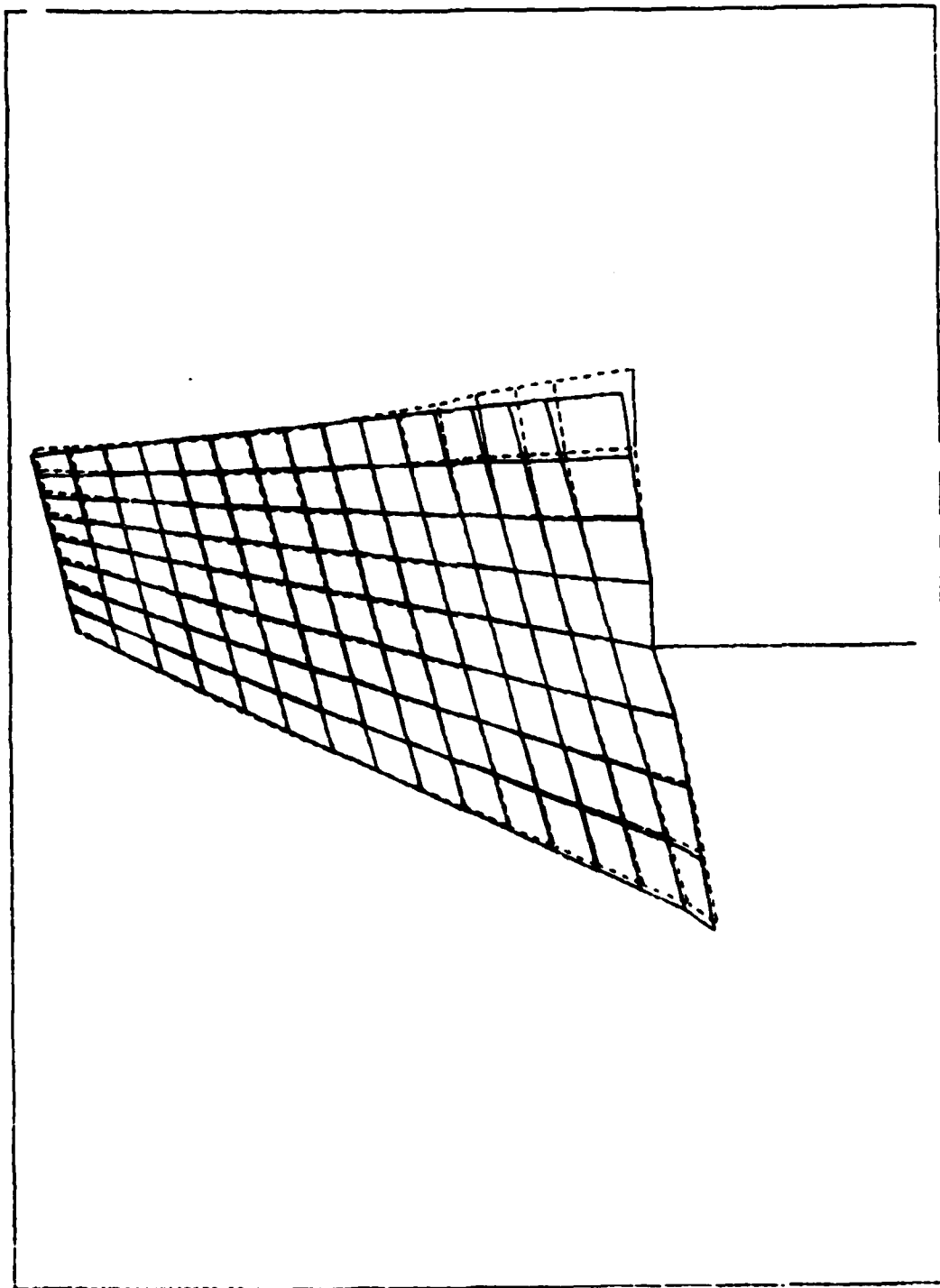


Figure 8 NASTRAN's 3rd Bending Mode, 124.68 cps

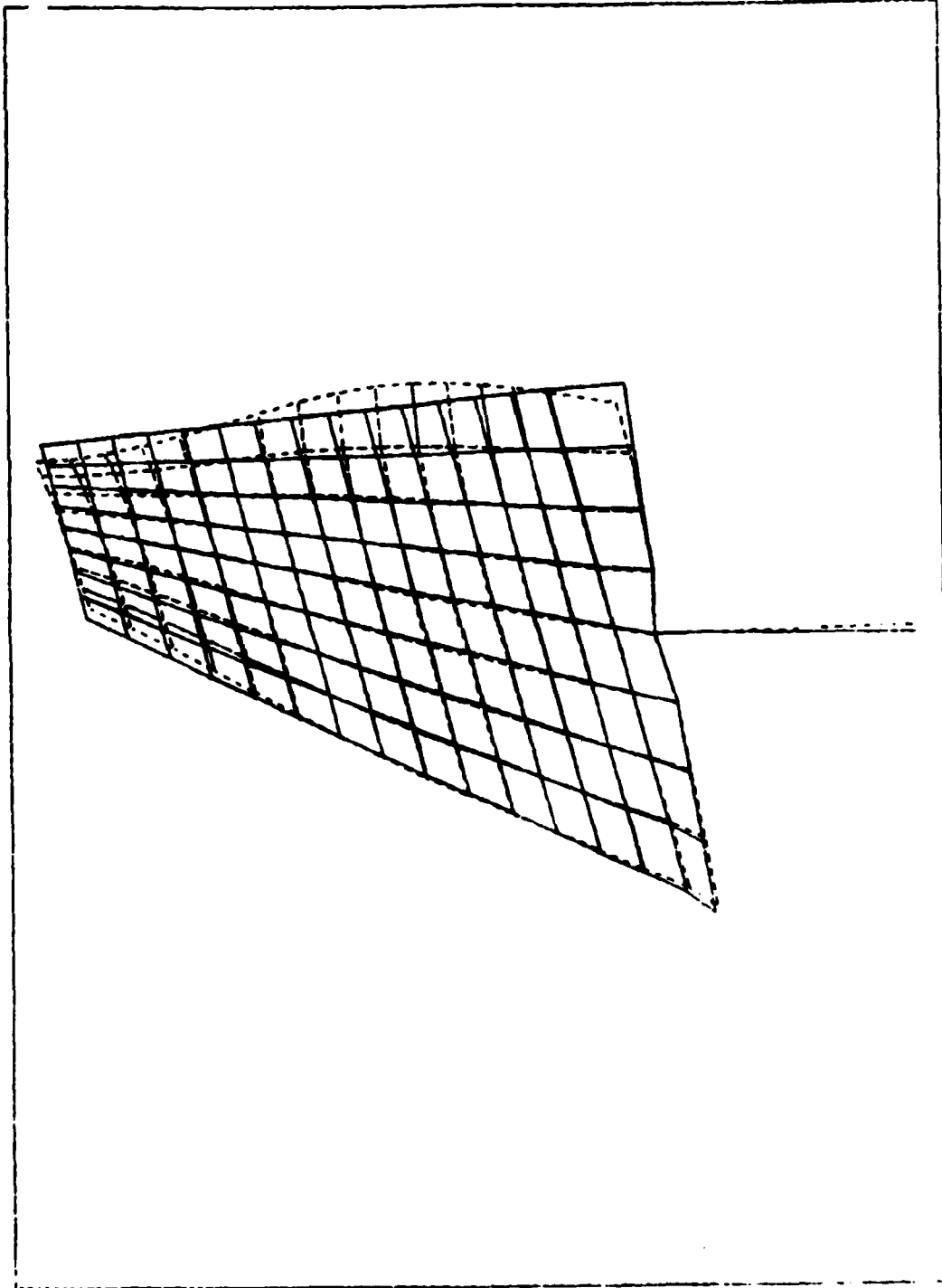
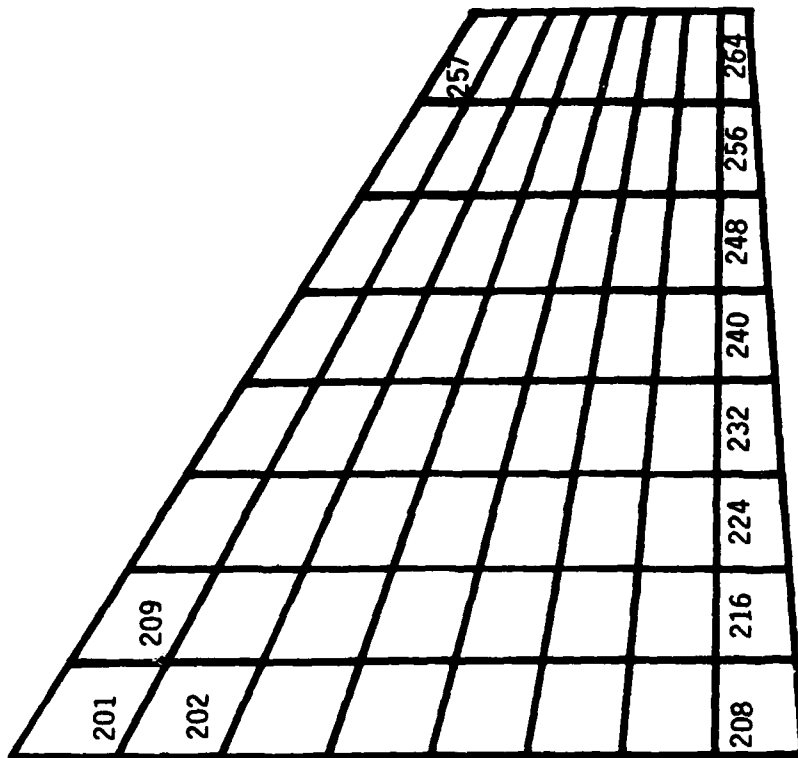


Figure 9 NASTRAN's 3rd Torsion Mode, 170.38 cps



— 64 Aerodynamic boxes numbered  
as shown.

Figure 10 8 b 8 Doublet Lattice Aerodynamic Model of the Stabilizer

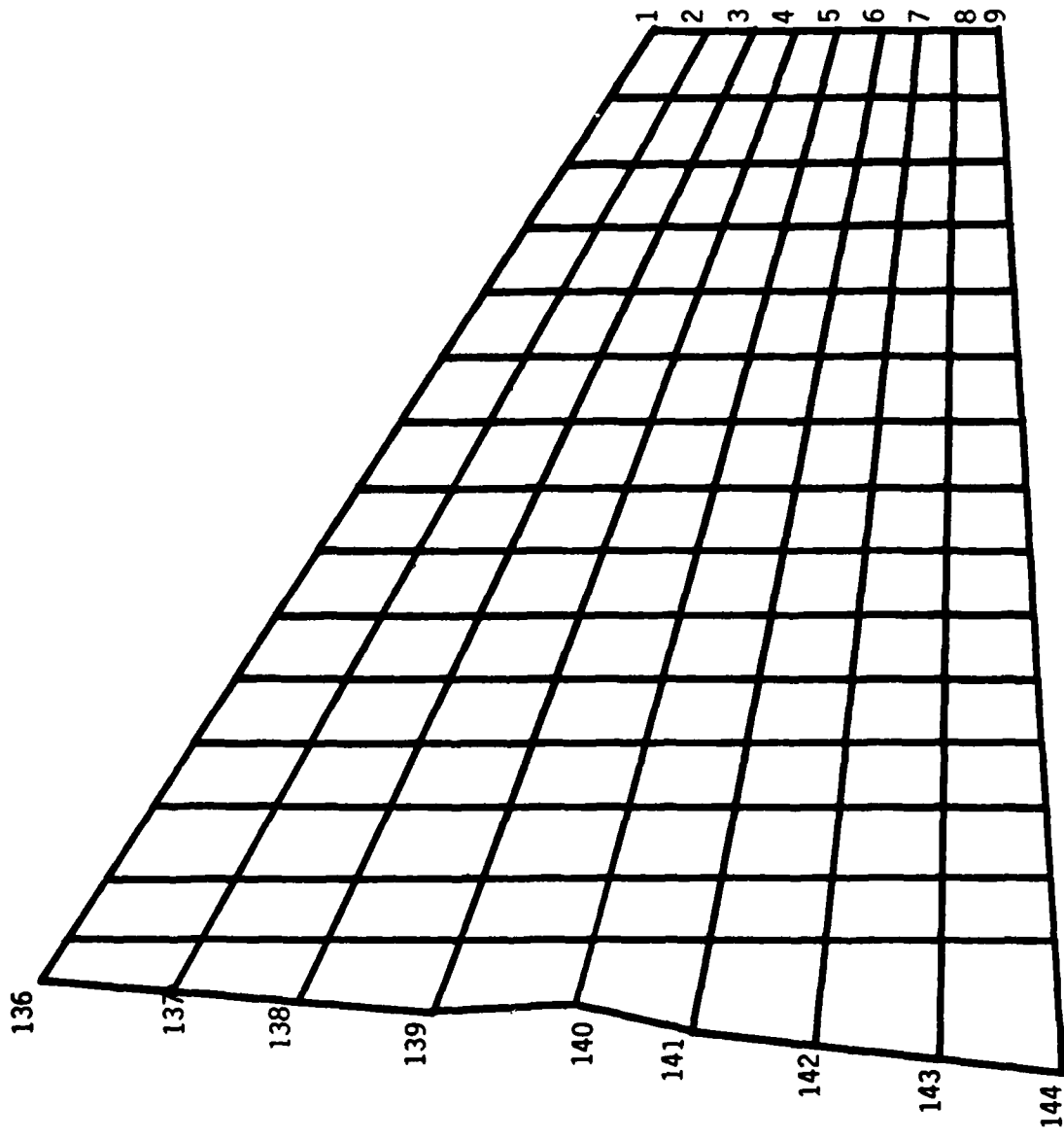


Figure 11 144 Grid Point Model for Input to the Spline

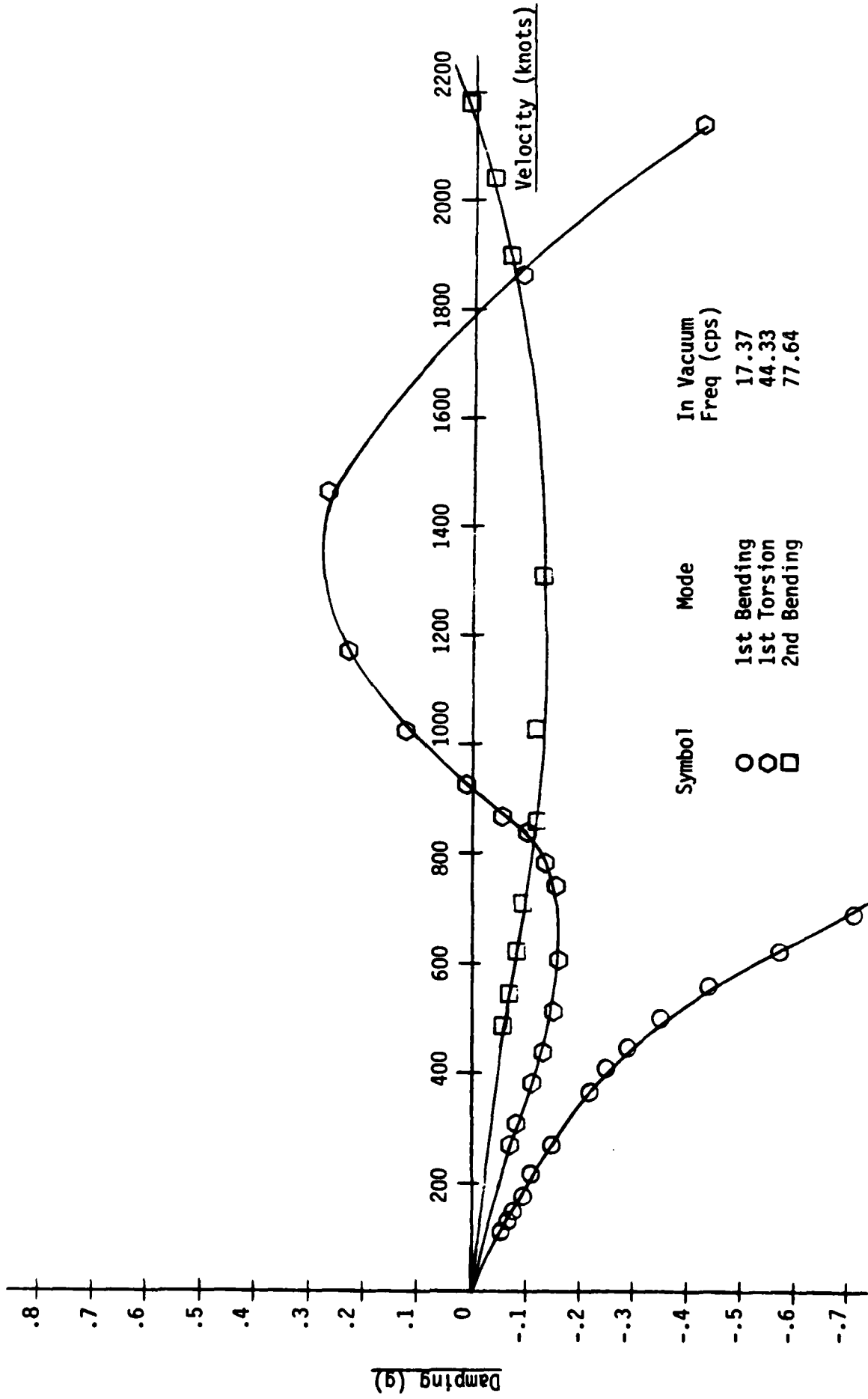


Figure 12 V-G Diagram of NASTRAN Computed First Three Modes

CHECKER
DATE

NORTHROP AIRCRAFT INC.

REPORT NO.
MODEL

FIGURE 22

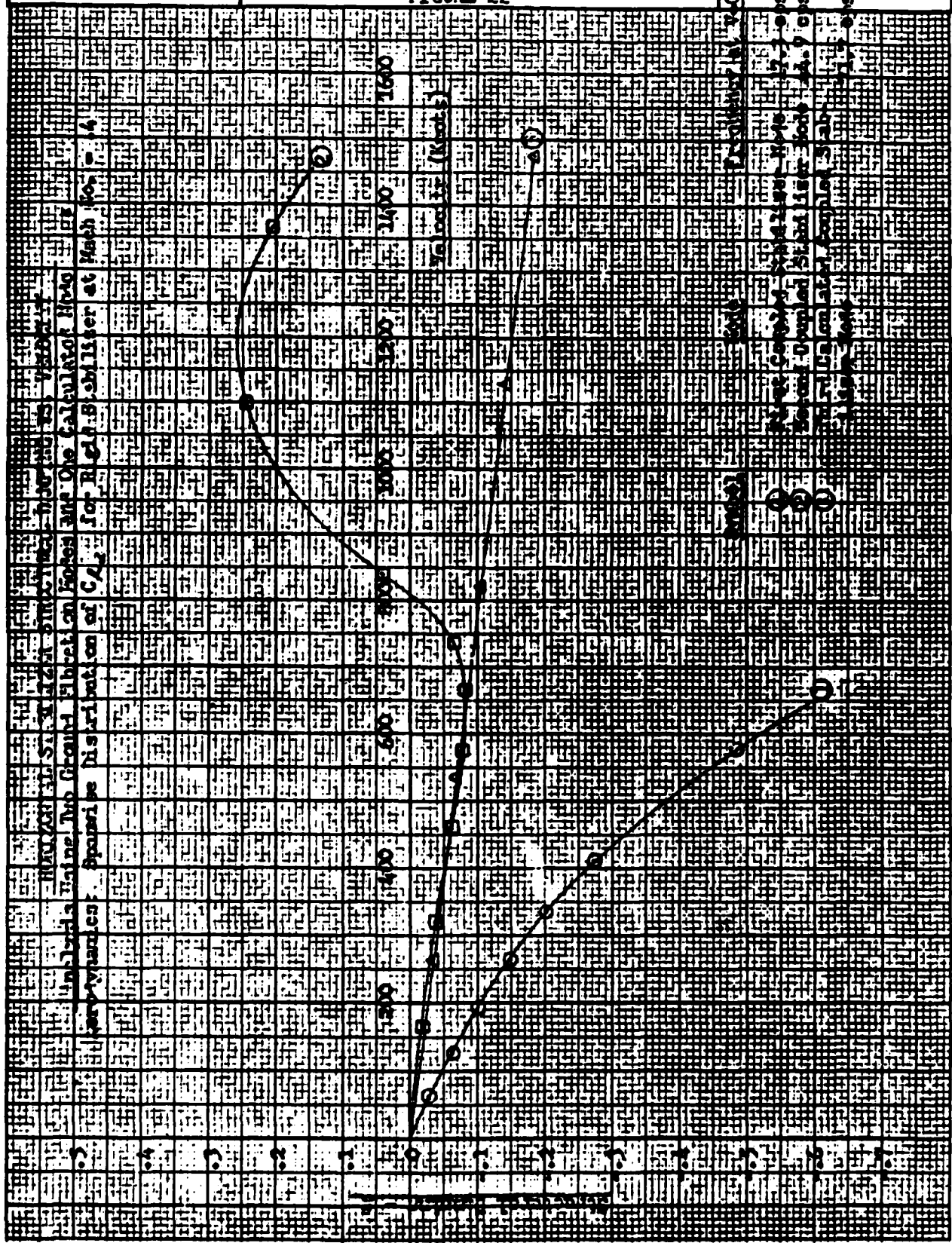
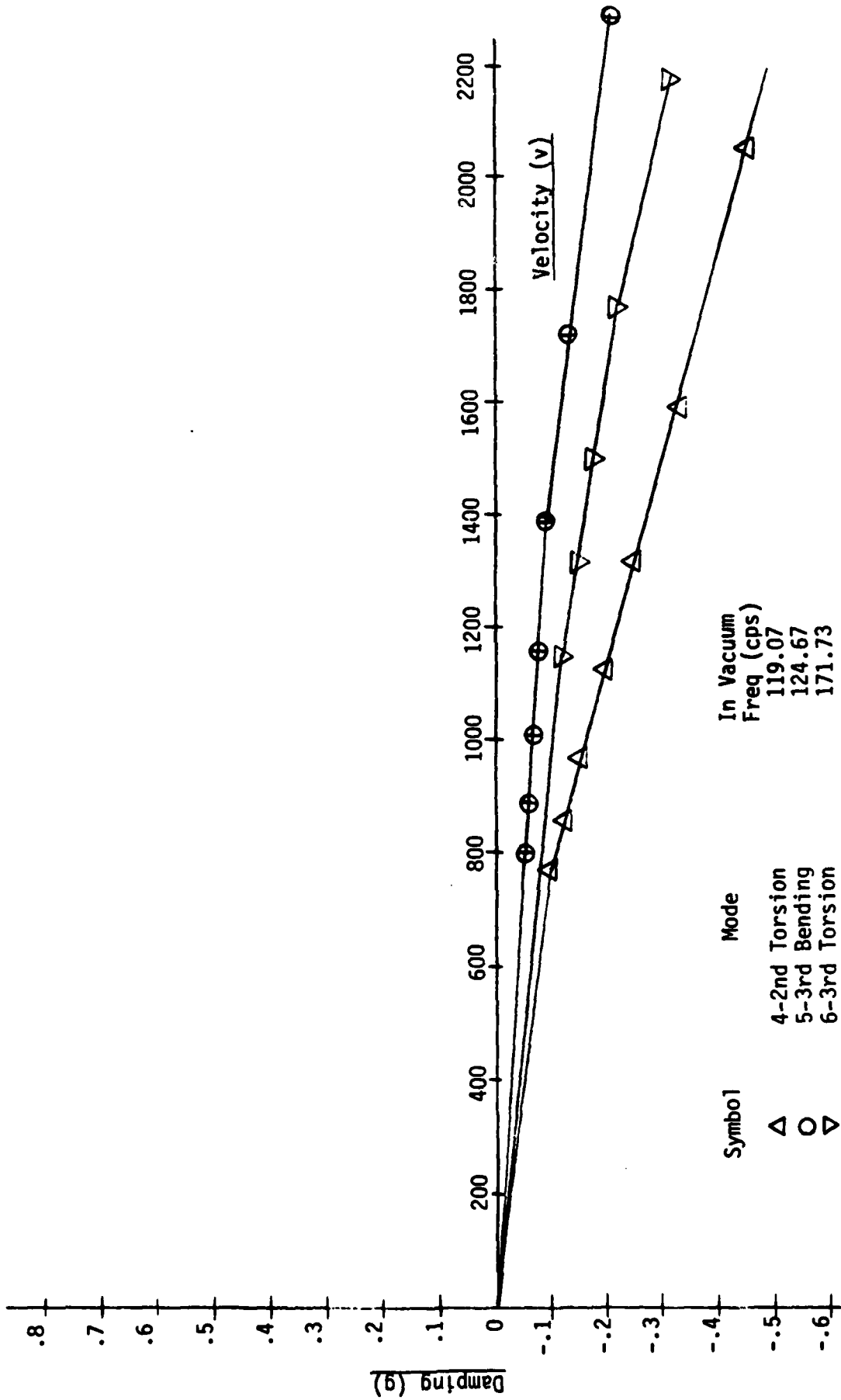


Figure 13 NAI's V-G Diagram of Computed First Three Modes (Ref 9)



Symbol	Mode	In Vacuum Freq (cps)
△	4-2nd Torsion	119.07
○	5-3rd Bending	124.67
▽	6-3rd Torsion	171.73

Figure 14 V-G Diagram of NASTRAN Computer Modes 4,5,6

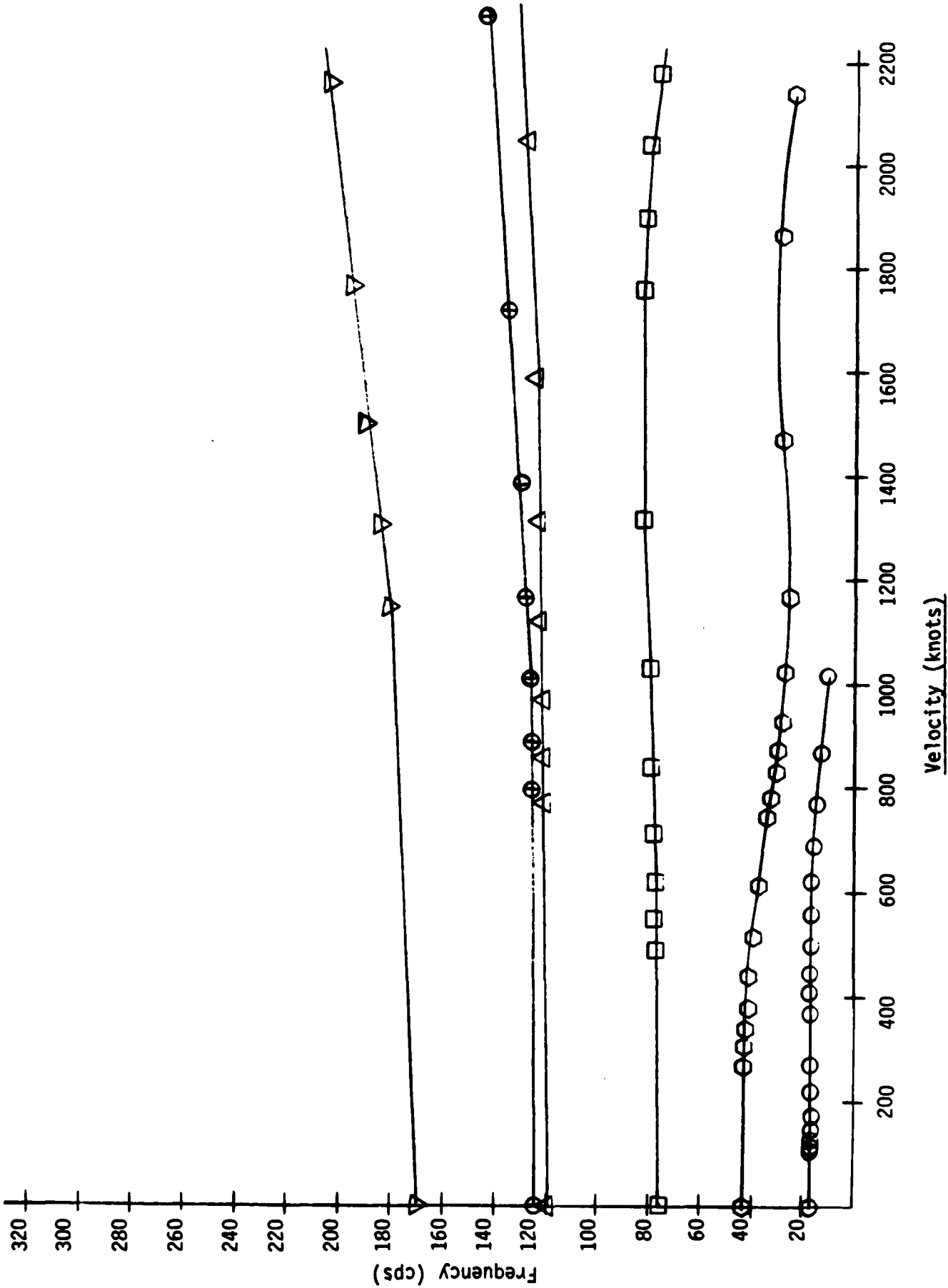


Figure 15 Frequency vs. Velocity, First 6 Modes

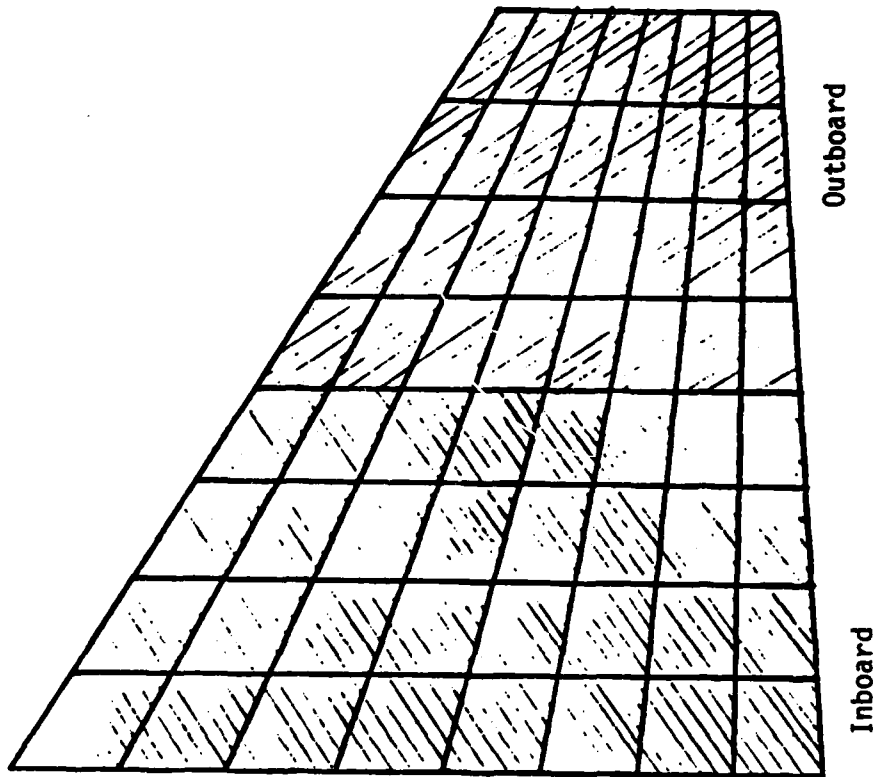


Figure 16 Segmented Spline, Two Sections

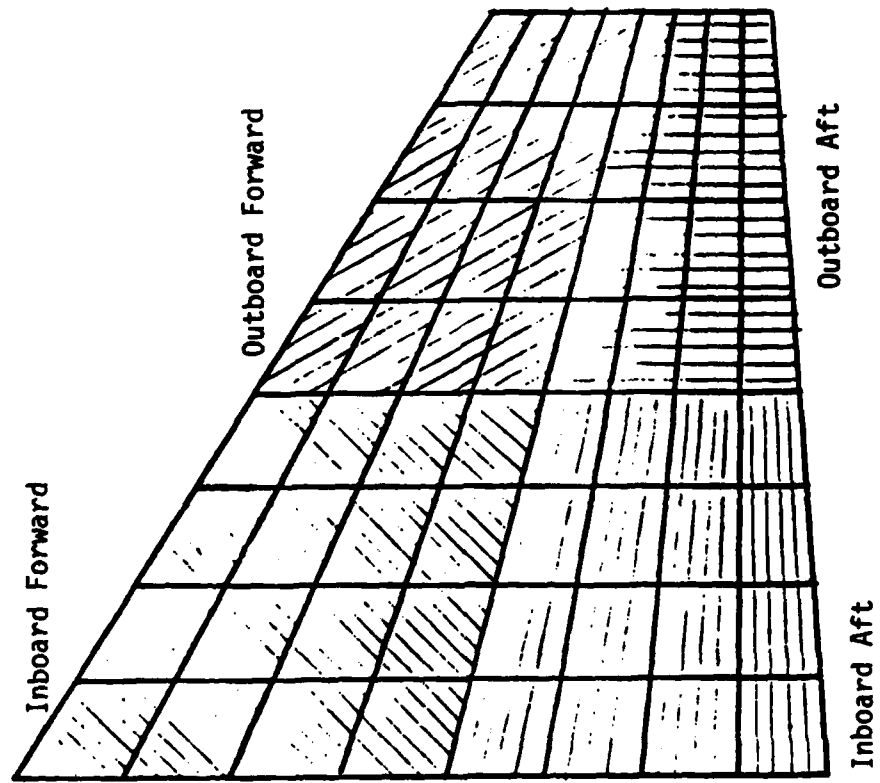


Figure 17 Segmented Spline, Four Sections

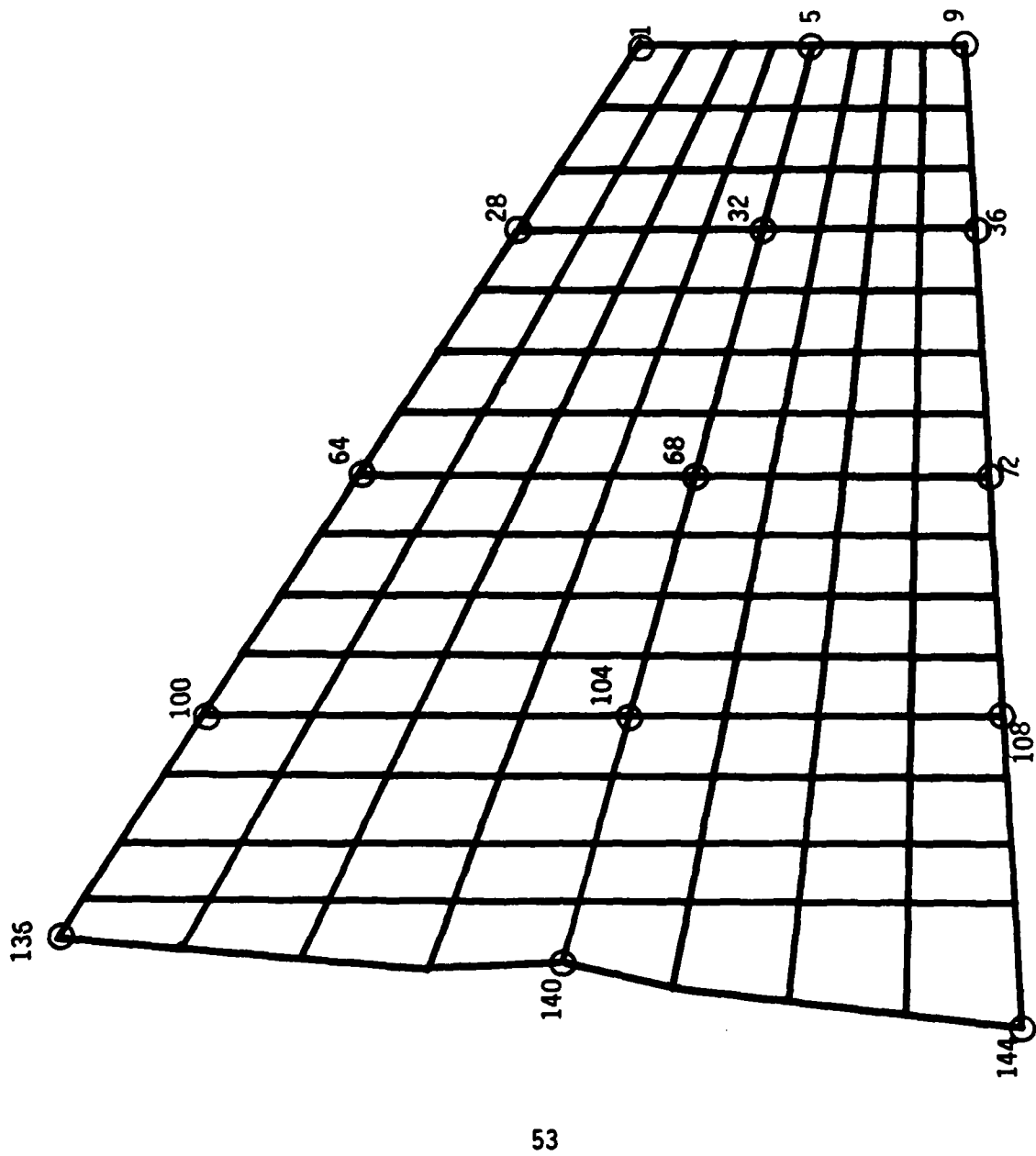


Figure 18 15 Structural Grid Point Model for Input to the Spline

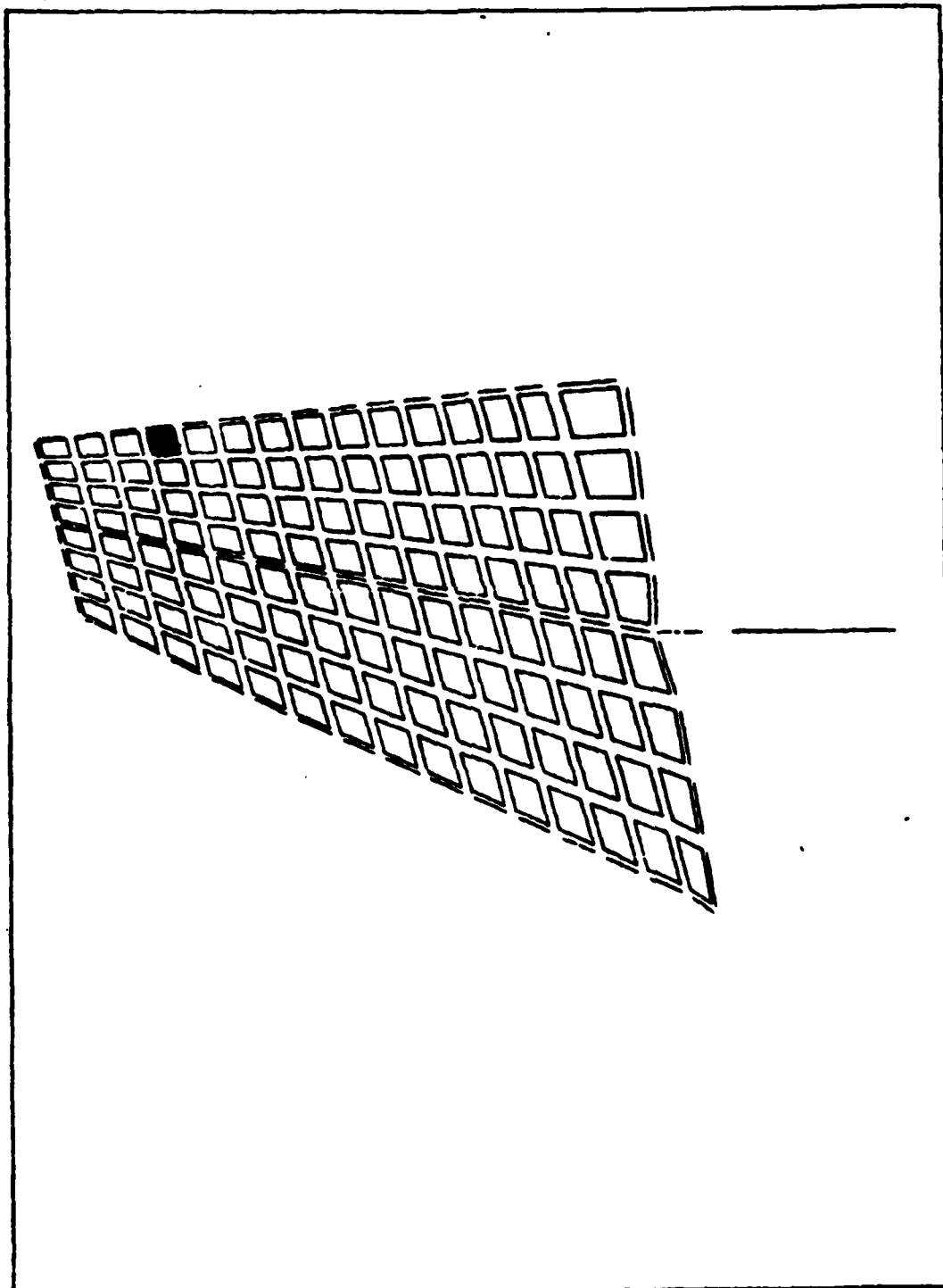


Figure 19 Simulated Repair, Hole Trailing Edge

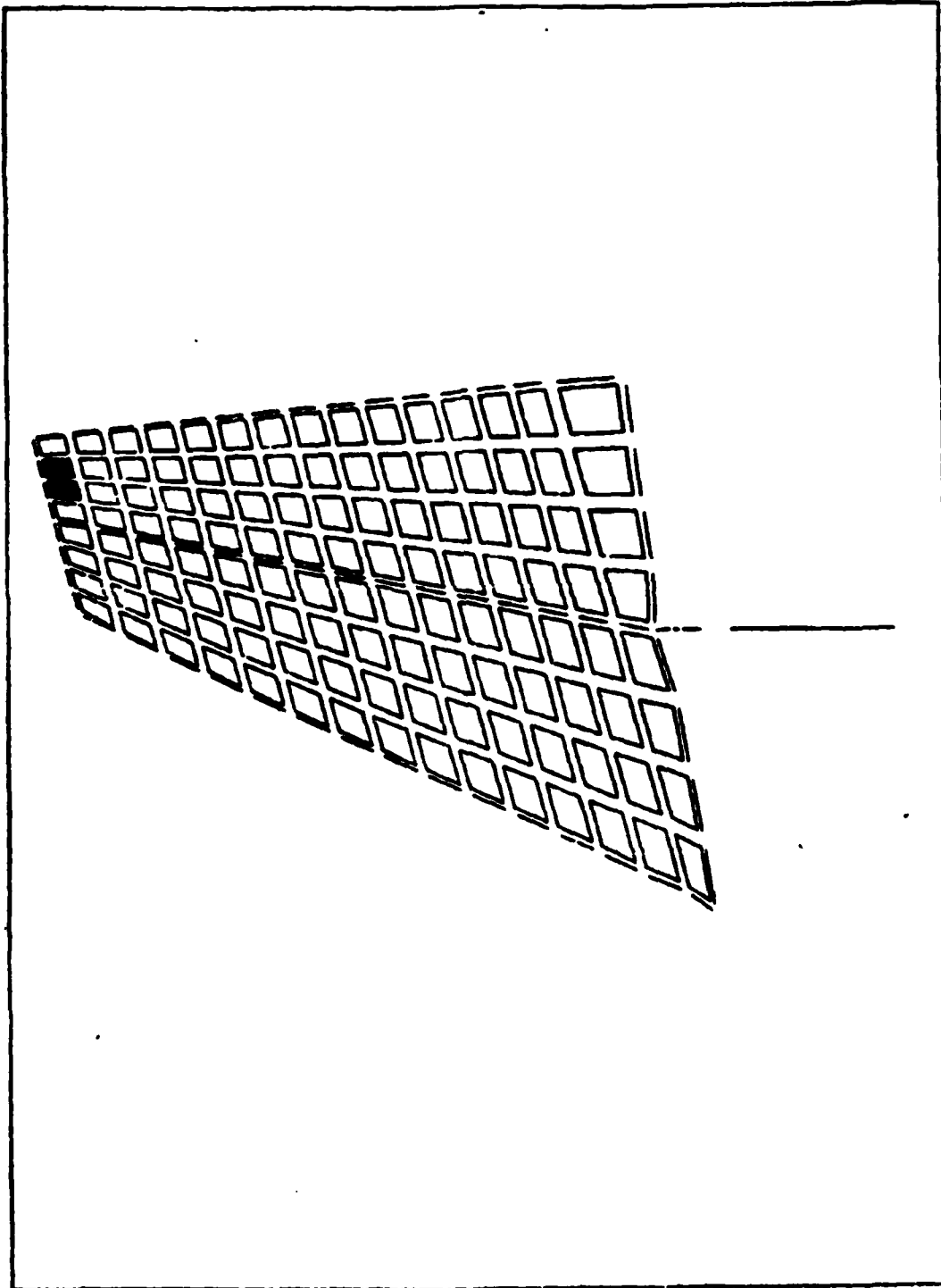


Figure 20 Simulated Repair, Hole Tip

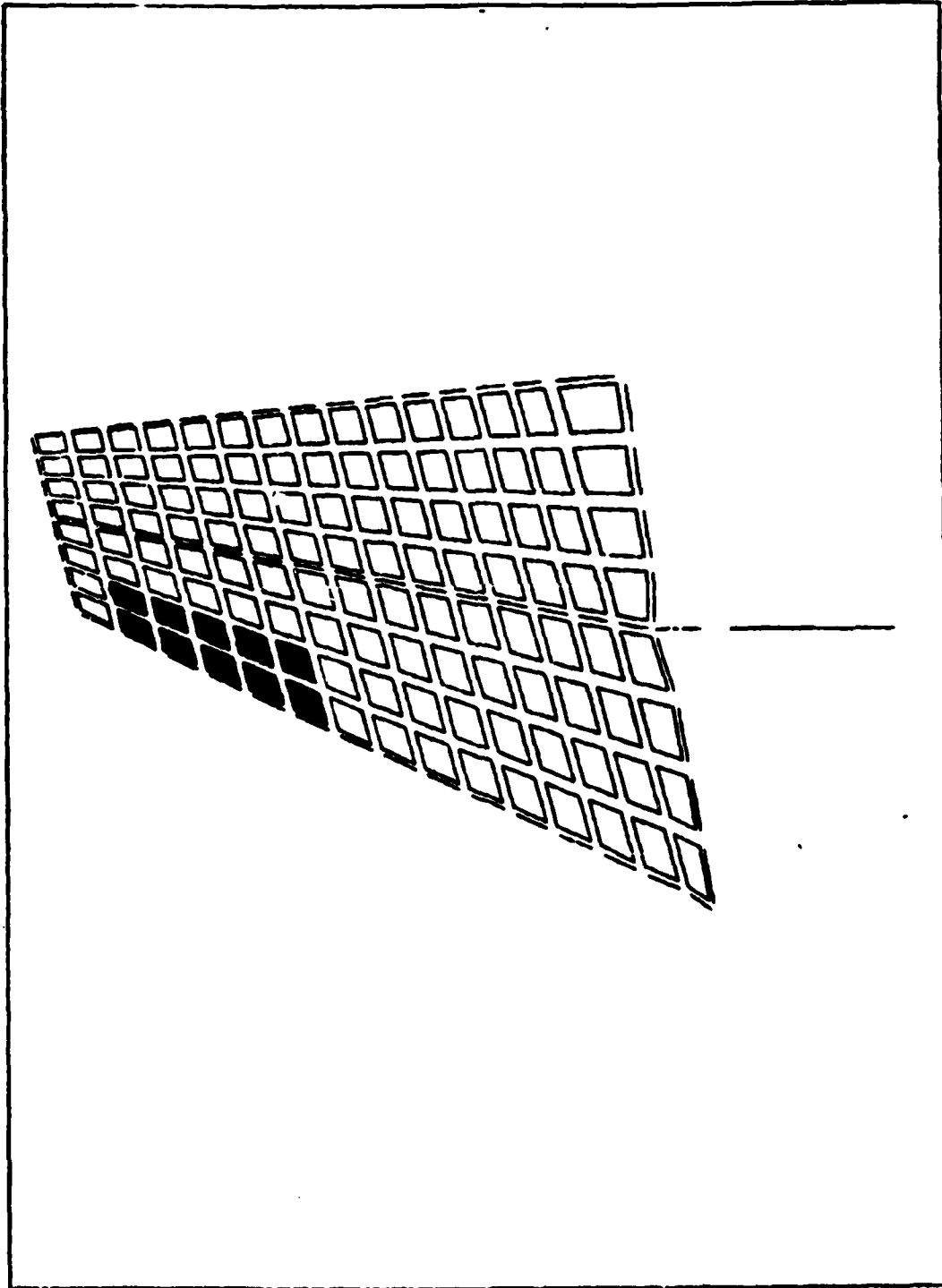
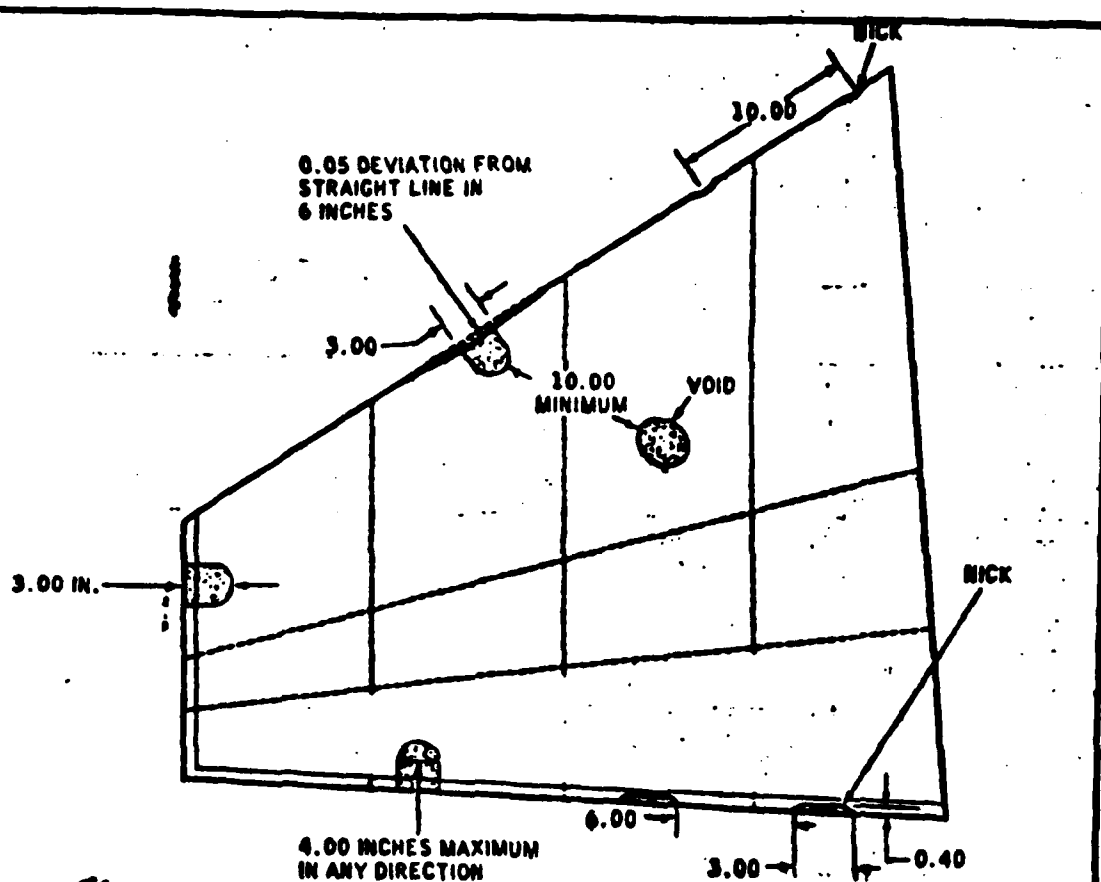


Figure 21 Simulated Repair, Delamination Leading Edge



*Note*  
REFER TO SECTION V.II  
FOR CLASSIFICATION OF  
HONEYCOMB DAMAGE.

ACCUMULATION OF DAMAGE LIMITS		
DENTS CLASS II		3 INCHES BETWEEN DAMAGE
DENTS CLASS III		SEE HOLE LIMITATIONS
VOID		2 REPAIRS ON EACH HORIZONTAL TAIL
SCRATCH CLASS III		SEE HOLE LIMITATIONS
NICK CLASS II	LEADING EDGE	10 INCHES MINIMUM
	CLOSING RIB	2 INCHES BETWEEN DAMAGE
	TRAILING EDGE	6 INCHES BETWEEN DAMAGE
BEND - TRAILING EDGE		1 REPAIR ON EACH HORIZONTAL TAIL
BREAK - TRAILING EDGE		10 INCHES BETWEEN EXTERNAL PATCH REPAIRS
CRACK CLASS II		SEE HOLE LIMITATIONS
HOLES		SEE SHEET 4
SCRATCH CLASS II		SEE SHEET 3
CORE RUPTURE		SEE HOLE LIMITATIONS

Figure 22 Repair Limit, Hole Trailing Edge (Ref 19)

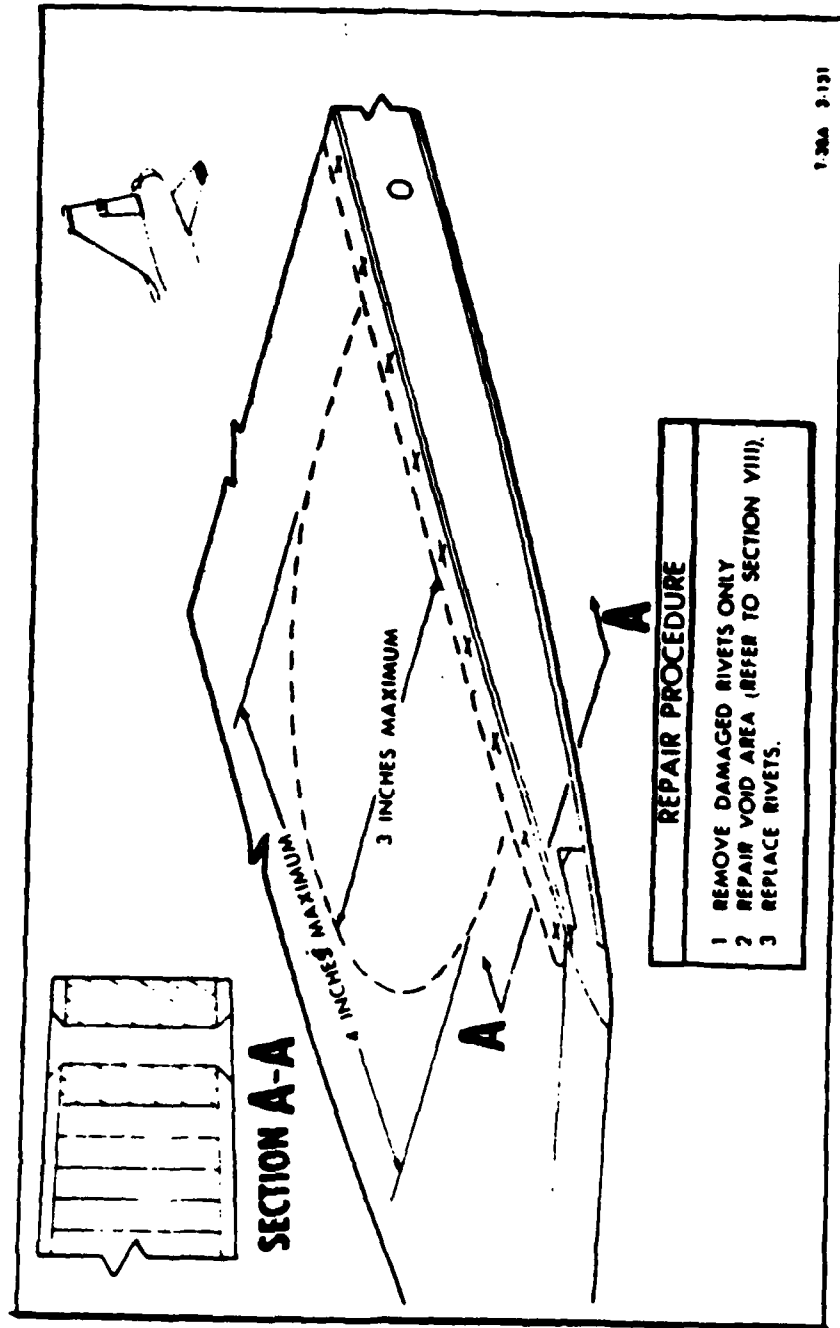


Figure 23 Repair Limit, Hole Tip (Ref 19)

## DELAMINATED EDGE AND CORRODED SKIN REPAIR

STEP

### 1 PREPARATION

ITEM

*Note*

① THIS REPAIR CAN BE USED FOR DAMAGE TO EITHER SKIN. THE MAXIMUM LENGTH OF AN INDIVIDUAL REPAIR IS 18 INCHES, PROVIDED THE LEADING EDGE EXTRUSION IS NOT REMOVED. THE REPAIR CAN EXTEND AFT FROM THE LEADING EDGE A MAXIMUM OF 6 INCHES. THE REPAIRS ILLUSTRATED ARE FOR DAMAGE TO ONE SKIN ONLY.

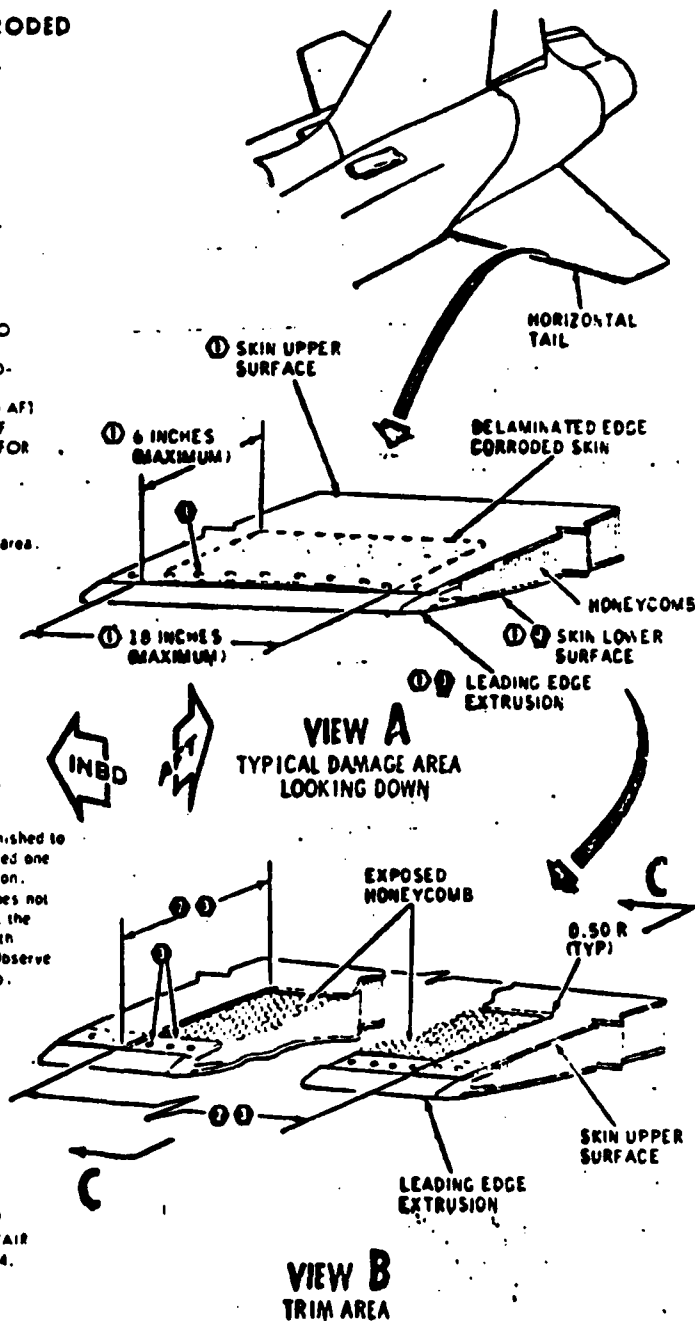
① Clean off all paint and primer from repair area. Remove rivets from corroded area.

② Cut corroded skin as shown in view B. Remove any corrosion from leading edge extrusion.

③ The surfaces of the extrusion may be burnished to a depth of 0.020, and or rivet holes may be reamed one attachment oversize if necessary to remove corrosion. If this procedure is not effective and repair area does not exceed the maximum limits of figure 4-4b, cut out the leading edge extrusion and repair in accordance with figure 4-4b. This will complete repair action. Observe 200 hours operating time limitation in figure 4-4b.

*Note*

\* IF REPAIR LIMITATIONS GIVEN IN ITEM ① ARE NOT EXCEEDED, CONTINUE WITH REPAIR PROCEDURES SHOWN ON SHEET 2, 3, OR 4.



1-28A 3-4-60

Figure 24 Repair Limit, Delamination (Ref 19)

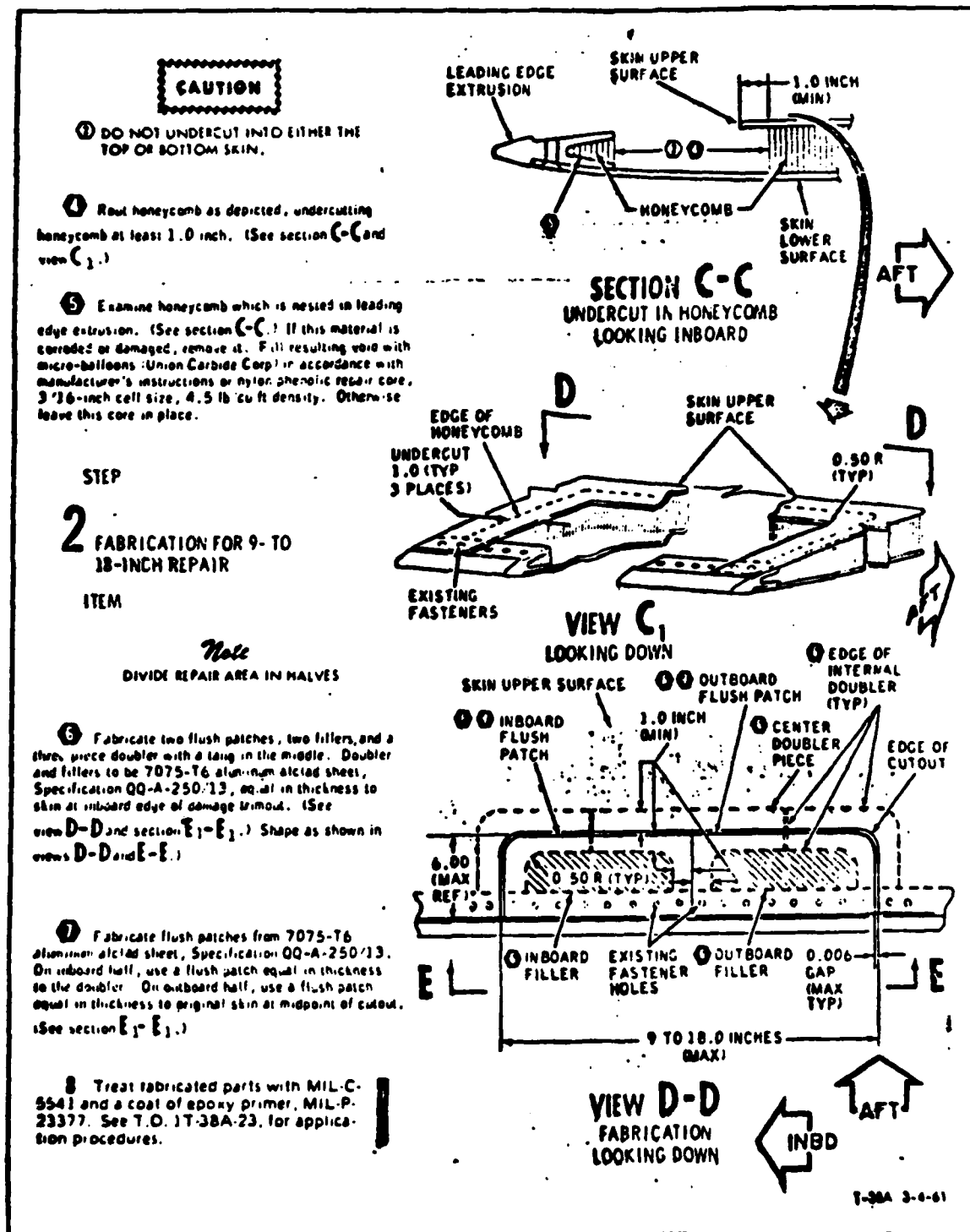


Figure 25 Repair Limit, Delamination (Ref 19)

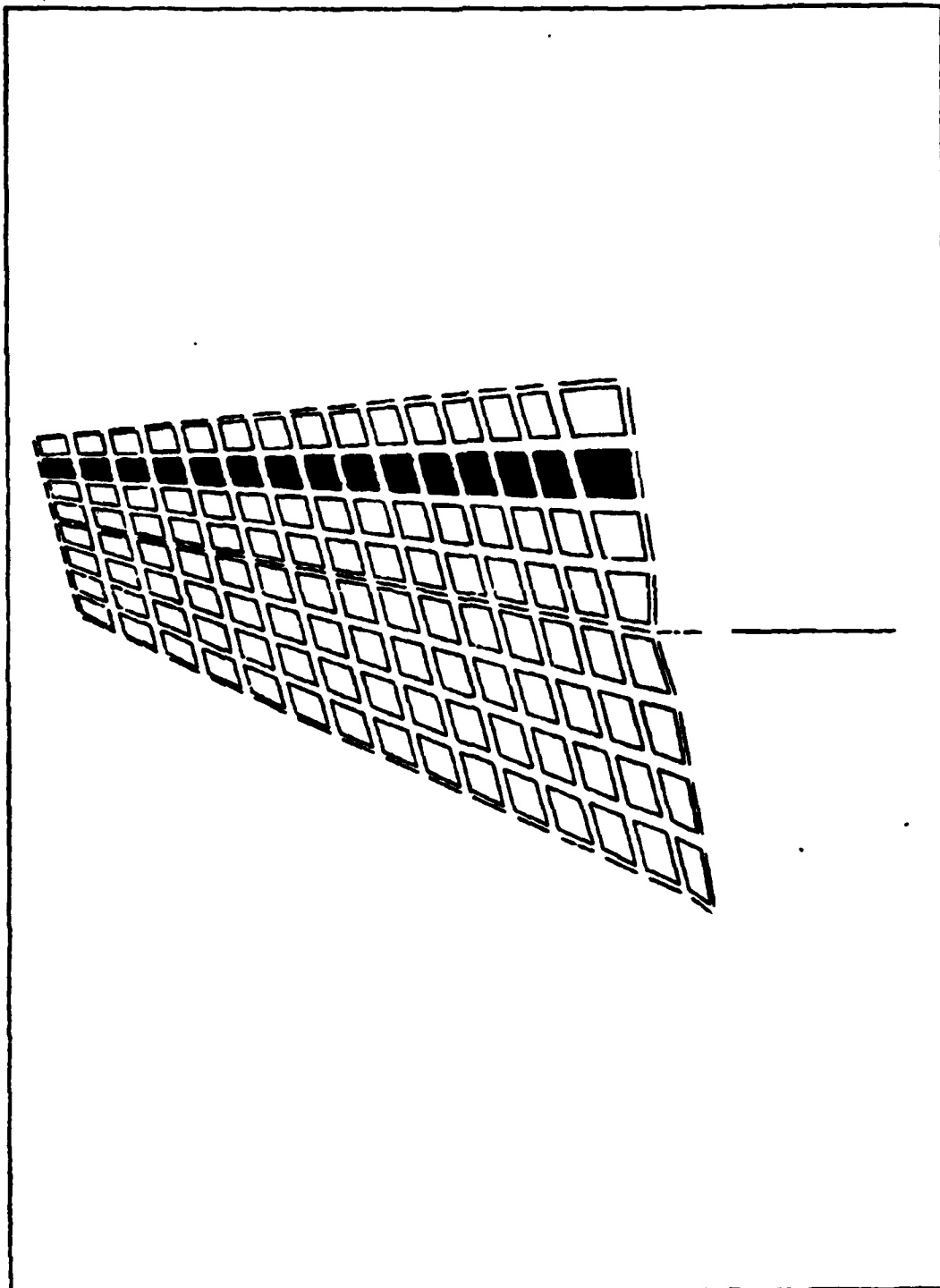


Figure 26 Simulated Repair Strip, Rib to Rib

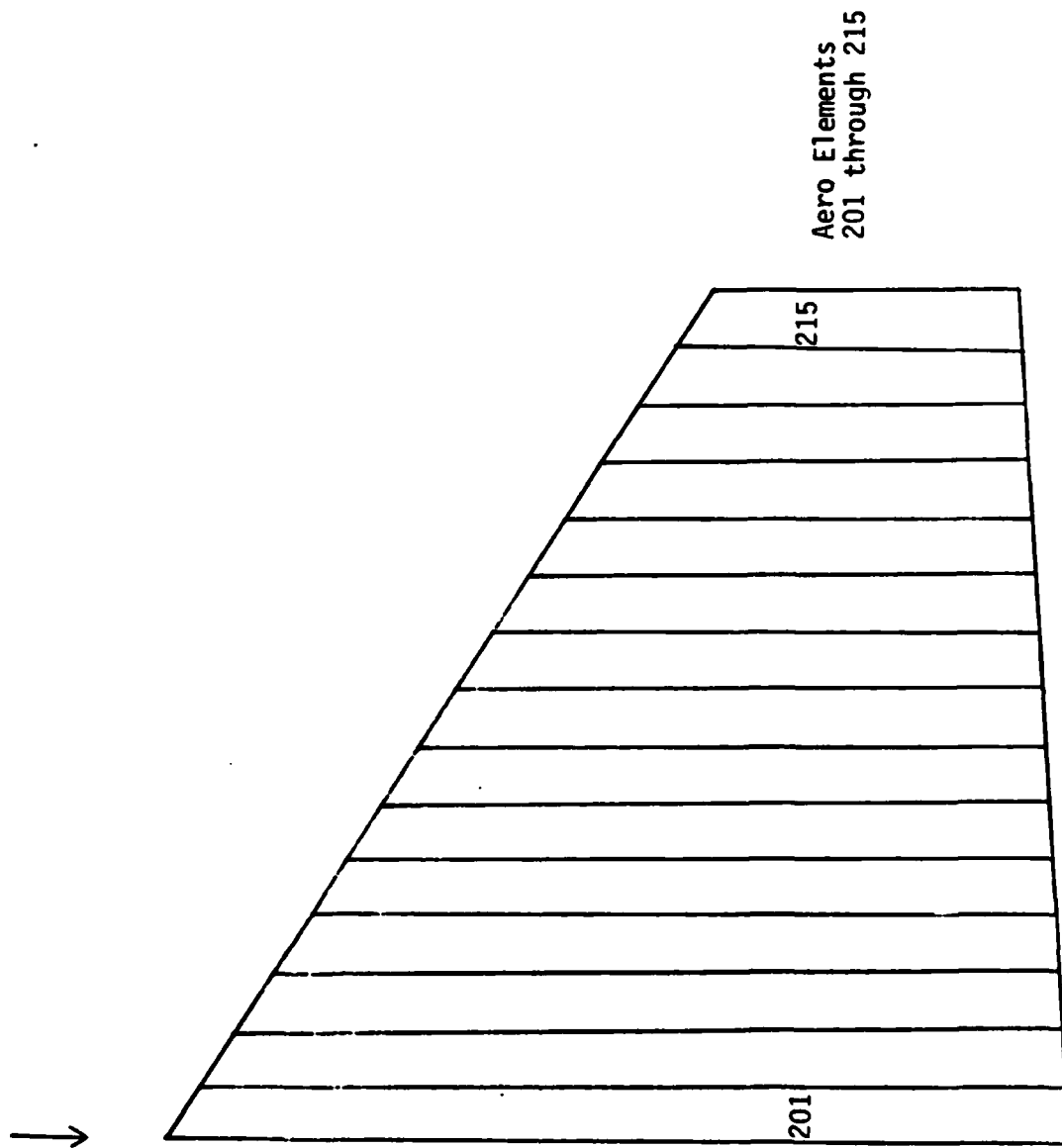


Figure 27 Strip Theory Aerodynamic Model of the Stabilizer

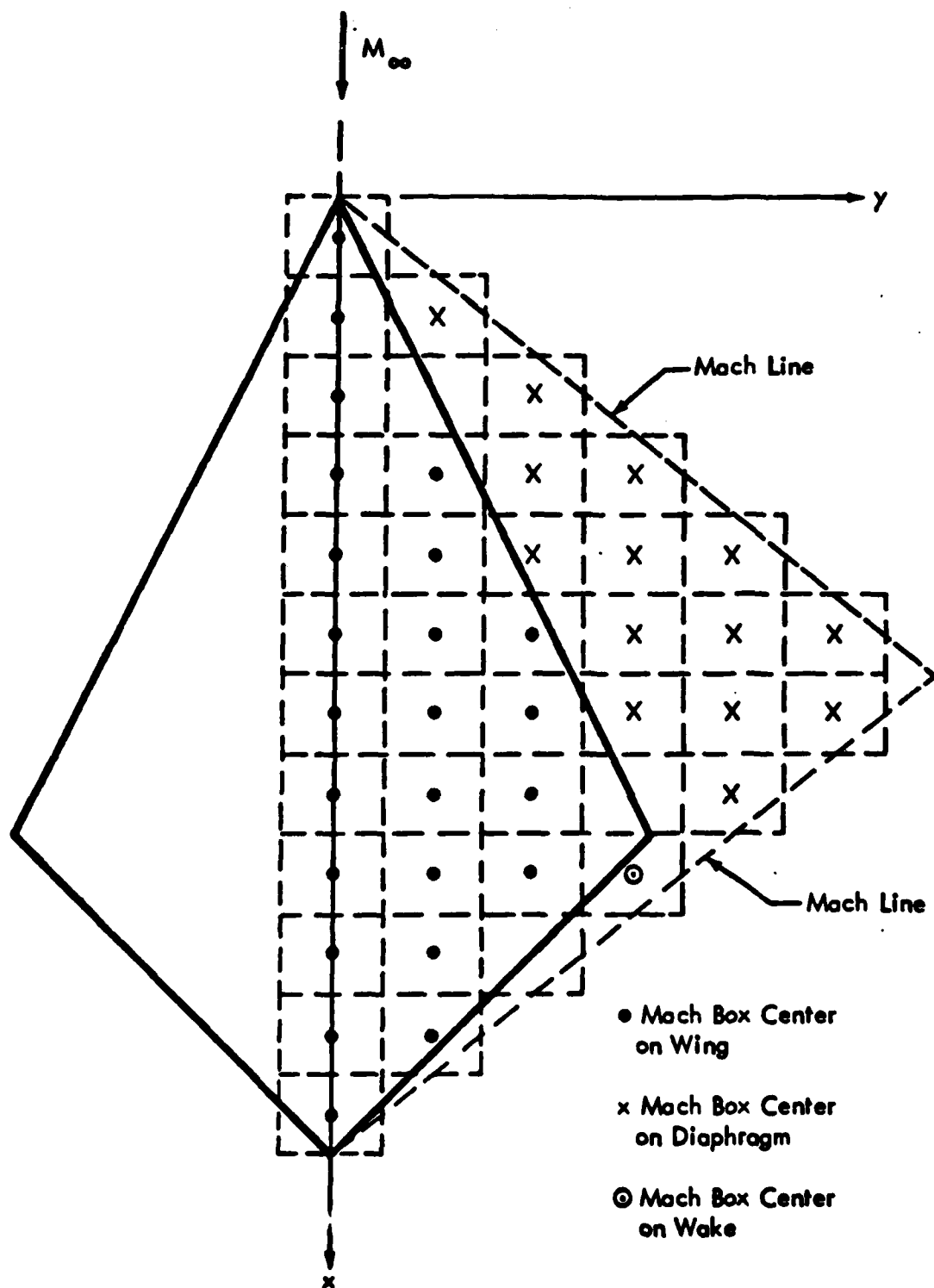


Figure 28 Regions of Typical Mach Box Aerodynamic Model (Ref 1)

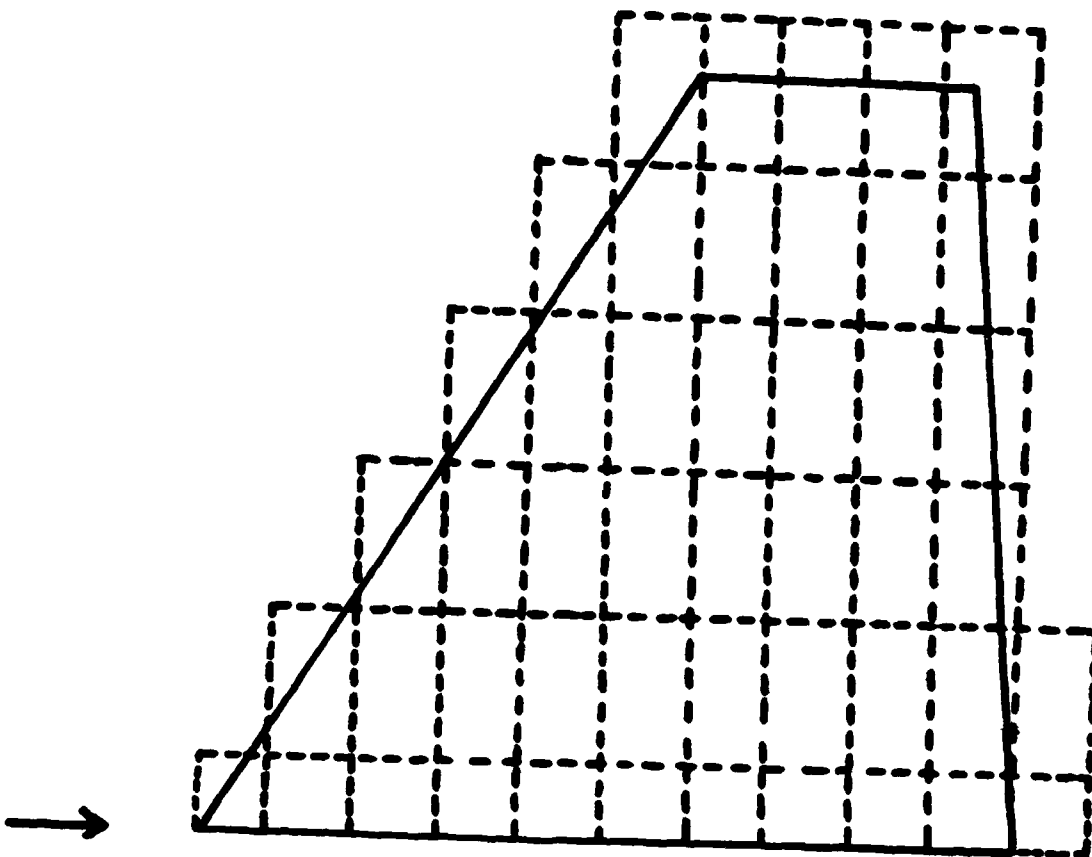
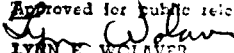


Figure 29 Mach Box Aerodynamic Model of the Stabilizer

## VITA

George Galloway London, Jr. was born on 19 May 1947 in Wilmington, North Carolina. He graduated from Williston Senior High School in Wilmington in 1965 and enlisted in the USAF in July 1965. He served tours of duty at Clark AB, Phillipines and Kadena AB, Japan in communications intelligence until his separation from active duty in May 1969 to attend college. He attended North Carolina Agricultural and Technical State University from which he received the degree of Bachelor of Science in Mechanical Engineering in June 1973. Upon graduation, he received a commission in the USAF through the ROTC program and entered pilot training at Webb AFB, Texas. He completed pilot training and received his wings in July 1974 and was selected to remain at Webb AFB as a T-38 instructor pilot. He then served as a C-141 pilot and flight instructor in the 6th Military Airlift Squadron, McGuire AFB, New Jersey. He was then selected to attend the School of Engineering, beginning June 1981, at the Air Force Institute of Technology, Wright-Patterson AFB, Ohio to earn a Master's Degree in Aeronautical Engineering. His next assignment after graduation is with the Foreign Technology Division, Wright-Patterson AFB, Ohio.

Permanent address: 520 Queen St.  
Wilmington, NC 28401

REPORT DOCUMENTATION PAGE		READ INSTRUCTIONS BEFORE COMPLETING FORM
1. REPORT NUMBER AFIT/GAE/AA/82D-19	2. GOVT ACCESSION NO. AD-A124741	3. RECIPIENT'S CATALOG NUMBER
4. TITLE (and Subtitle) Investigation of an Improved Finite Element Model for a Repaired T-38 Horizontal Stabilizer Flutter Analysis Using NASTRAN		5. TYPE OF REPORT & PERIOD COVERED MS Thesis
		6. PERFORMING ORG. REPORT NUMBER
7. AUTHOR(s) George G. London, Jr.		8. CONTRACT OR GRANT NUMBER(s)
9. PERFORMING ORGANIZATION NAME AND ADDRESS Air Force Institute of Technology (AFIT/EN) Wright-Patterson AFB, OH 45433		10. PROGRAM ELEMENT, PROJECT, TASK AREA & WORK UNIT NUMBERS
11. CONTROLLING OFFICE NAME AND ADDRESS		12. REPORT DATE December 1982
		13. NUMBER OF PAGES 73
14. MONITORING AGENCY NAME & ADDRESS (if different from Controlling Office)		18. SECURITY CLASS. (of this report)  Unclassified
		15a. DECLASSIFICATION/DOWNGRADING SCHEDULE
16. DISTRIBUTION STATEMENT (of this Report)  Approved for public release; distribution unlimited.		
17. DISTRIBUTION STATEMENT (of the abstract entered in Block 20, if different from Report)		
18. SUPPLEMENTARY NOTES		Approved for public release: INW AFR 100 17.  LYNN E. WCLAVER Dean for Research and Professional Development Air Force Institute of Technology (AIO) Wright-Patterson AFB OH 45433
19. KEY WORDS (Continue on reverse side if necessary and identify by block number) NASTRAN Structural Model Aerodynamic Model Stabilizer Mode Shape Flutter Analysis		
20. ABSTRACT (Continue on reverse side if necessary and identify by block number) This thesis investigated the use of an improved finite element model of a T-38 horizontal stabilizer for flutter analysis using NASTRAN. The procedure for evaluating the effect of repairs on the flutter speed is developed and its sensitivity to several modeling assumptions and practices is presented. The procedure is to be used by Air Force engineers to evaluate repair limits of T-38 stabs. The NASTRAN flutter speed calculations are based upon a structural model, an unsteady aerodynamic model, and an interface model (splines). The structural		

UNCLASSIFIED

SECURITY CLASSIFICATION OF THIS PAGE (When Data Entered)

model consists of a flat array of plates and bars representing the single spar honeycomb structure. A flat array of doublet lattice panels were chosen for the unsteady aerodynamic model. An interface between these two models is required to find the down washes on the aerodynamic model due to motion of the structural model. This is accomplished by interpolation via surface splines.

Variations in the input parameters were considered to determine their effect on the flutter conditions. In addition to using the doublet lattice method, strip theory and mach box methods were used in the flutter analysis. This allowed a comparison of flutter conditions versus aerodynamic theory to be made.

The results show that the current repair limits have little or no effect on the flutter conditions, therefore, the procedures presented in this investigation should be used to establish new repair limitations.

UNCLASSIFIED

SECURITY CLASSIFICATION OF THIS PAGE (When Data Entered)

**END**

**FILMED**

**3-83**

**DTIC**